Supplementary Materials for

The Chemical Structure of Widespread Microbial Aryl Polyene Lipids

Authors: Gina L. C. Grammbitter[1]‡, Yi-Ming Shi[1]‡, Yan-Ni Shi[1]‡, Sahithya P. B. Vemulapalli[2]‡, Christian Richter[3], Harald Schwalbe[3], Mohammad Alanjary[1,4], Anja Schüffler[5], Matthias Witt[6], Christian Griesinger[2], Helge B. Bode* [1, 7, 8, 9].

Affiliations:

[1] Institute of Molecular Biological Science, Johann Wolfgang Goethe University, 60438 Frankfurt, Germany.

[2] Max Planck Institute for Biophysical Chemistry, NMR-based Structural Biology, 37077 Göttingen, Germany.

[3] Institute for Organic Chemistry and Chemical Biology, Center for Biomolecular Magnetic Resonance, Johann Wolfgang Goethe University, 60439 Frankfurt am Main, Germany.

[4] Bioinformatics Group, Wageningen University, Droevendaalsesteeg 1, 6708PB Wageningen, Netherlands.

[5] University of Kaiserslautern, Paul-Ehrlich-Str. 23, 67663 Kaiserslautern, Germany.

[6] Bruker Daltonik GmbH, Fahrenheitstrasse 4, 28359 Bremen, Germany.

[7] Senckenberg Gesellschaft für Naturforschung, Frankfurt am Main, 60325, Germany.

[8] Buchmann Institute for Molecular Life Sciences (BMLS), Johann Wolfgang Goethe University, Max-von-Laue-Straße 15, 60438 Frankfurt am Main, Germany.

[9] Max-Planck-Institute for Terrestrial Microbiology, Department of Natural Products in Organismic Interactions, 35043 Marburg, Germany.

*Correspondence to: helge.bode@mpi-marburg.mpg.de.

‡These authors contributed equally.

This PDF file includes:

Materials and Methods
Figs. S1 to S17
Tables S1 to S11

Materials and Methods

Cloning. Genomic DNA from *X. doucetiae* was isolated using the Gentra Puregene Yeast/Bact kit (Qiagen). Polymerase chain reaction was (PCR) performed with Phire Hot Start II DNA polymerase (Thermo Scientific), Phusion High-Fidelity DNA Polymerase, or Q5 polymerase (New England Biolabs) according to the manufacturer's instructions. Oligonucleotides were purchased from Eurofins Genomics. The *Invisorb Spin DNA Extraction Kit* (Stratec) was used for DNA purification from agarose gels following the manufacturer's protocol. Plasmids were isolated with the Invisorb Spin Plasmid Mini Two Kit (Stratec). Plasmid backbone PCRs with pEB17 were performed using the oligonucleotide pair GG23 and GG138. The backbone PCR was restriction digested with *Dpn*I (New England Biolabs) and cleaned-up again with the *Invisorb Spin DNA Extraction Kit* (Stratec). All plasmids (Table S3) were cloned via a two-fragment based Hot Fusion reaction.[1] The corresponding oligonucleotides used for insert and backbone PCRs are listed in Table S2. *E. coli* ST18λpir was used as a cloning strain and electroporated with the desalted (MF-Millipore membrane, VSWP, 0.025 µm) Hot Fusion reaction. Kanamycin was used in a final concentration of 50 µg/mL.

Construction of Single Deletion Mutants. Deletions of single genes *apeB* to *apeR* (Table S4) in the *ape*$^+$ (*X. doucetiae*Δ*DC*Δ*hfq*P_{BAD}*apeB*) were constructed as described previously.[2] Briefly, the *ape*$^+$ strain was conjugated with an *E. coli* ST18 strain, harboring the corresponding deletion plasmid with 500-900 bp of the up- and downstream flanking regions of the gene of interest (Table S3). In a first homologous recombination event, the pEB17 plasmid is inserted into the *Xenorhabdus* genome and maintained by kan^R selection. Therefore, both strains were grown in 10 mL LB-medium (10 g/L tryptone, 5 g/L yeast extract, and 5 g/L NaCl at pH 7.5) (*E. coli* ST18-λpir was supplemented with 50 µg/mL kanamycin and δ-aminolevulinic acid) to an OD_{600} of 0.6-

0.8 and harvested in a ratio of 5:1 (5 mL *X. doucetiae* strain:1 mL *E. coli* strain). To deplete δ-aminolevulinic acid, the *E. coli* ST18λpir pellet was washed three times with 1 mL LB. Cells were resuspended in 60-90 µL LB and mixed before pipetting them in one drop (90 µL) on an LB agar plate. After 1 d at 30°C, cells were resuspended in 1 mL LB liquid medium and 200 µl of the suspension was plated on LB agar plates containing kanamycin. For generation of the deletion mutants, single colonies of the kanamycin-resistant clones were grown on LB agar plates containing 12% (w/v) sucrose resulting in a loss of the plasmid backbone.

The deletion mutants were verified by colony-PCR using oligonucleotides listed in Table S2. Briefly, half of a colony of the corresponding mutant was picked and resuspended in 50 µL 1x taq-buffer and heated in the microwave (600 W) for 3 min. 1 µL of the resulting cell suspension was used for a 25 µL PCR-reaction (10 µM oligonucleotide fw/rv, 10 mM dNTPs, 1x taq-buffer, 0.25 µL taq) using Taq DNA polymerase (New England Biolabs) according to the manufacturer's protocol. The resulting strains are listed in Table S1.

Cultivation and Small Scale Extraction of *ape*$^+$ and Mutant Strains. All strains were cultivated in 30 mL LB medium (300 mL flasks) at 30°C with 150 rpm for 48 h. Therefore, the strains were inoculated with an overnight preculture to an OD_{600} of 0.1 and supplemented with 0.2% L-arabinose (from 20% L-arabinose stock solution in water). APELs were extracted from the cell-pellet (centrifugation for 10 min at 10 000 x *g*), with 15 mL DCM:MeOH for 30 min at 30°C. The filtered crude extract was evaporated to dryness under vacuum and again resuspended in 1 mL DCM/MeOH for HPLC-MS analysis. The HPLC-UV/MS analysis of APEL compounds was performed as described below and with the conditions listed in Table S5.

^{13}C- and ^{15}N-labeling with the *ape*$^+$ Mutant *ΔapeB*. Isotope labeling experiments were performed in 30 mL of fully ^{13}C or ^{15}N labeled ISOGRO medium (Sigma Aldrich) as described

previously.[3] Cultivation, extraction, and HPLC-MS analysis of the *ape*$^+$ mutant *ΔapeB* was carried out as described above.

GC-MS Analysis of APEL FAMEs. To detect the FA moieties of the pure APEL-1284 (**1**), 1270 (**2**), 1256a (**3**), and 1242 (**4**), the fatty acid methyl ester (FAME) derivatization protocol and GC-MS conditions were used.[4]

Thin-Layer Chromatography of APEL Extracts. Thin-layer chromatography for phospholipids was performed as described.[5]

HPLC-UV/(HR)ESI-MS Analysis of APELs. The crude extract of the *ape*$^+$ and the *ape*$^+$ mutants *ΔapeB-R* were analyzed via high resolution HPLC-UV/(HR)ESIMS analysis using a Dionex Ultimate 3000 LC system (Thermo Fisher), equipped with a DAD-3000 RS UV-detector (Thermo Fisher), coupled to an Impact II electrospray ionization mass spectrometer (Bruker). Internal mass calibration was achieved by injecting a 10 mM sodium formate solution (0-1.5 min, calibration segment).

Unless otherwise specified, injection volumes were 5-20 µL. Columns, solvent system (used according to[6]), and LC- and MS-parameter are listed in Table S5. For Data analysis of HPLC-UV/MS-chromatograms, Compass DataAnalysis 4.3 (Bruker) was used.

MR-MS Analysis of Purified APELs. The measurements were performed with a scimaX 7T MR-MS system, equipped with an Apollo II Dual ESI/MALDI source. The ESI source was used in positive mode with a mass detection range of *m/z* 107-2000. Spectra were acquired in quadrupolar phase detection, with a resolving power of 650.000 at *m/z* 400. Mass calibration was achieved externally with a NaTFA cluster. For measurement of the exact mass of precursor masses and fragment masses in CID spectra, the lock mass 622.02896 was used (Collision energy: 25 eV). For

sample measurement, stock solutions of the samples were prepared in DCM:MeOH (1:1) at a concentration of 1 mg/mL. The stock solutions were diluted 1:20 in 98% MeOH/2% water (+10 mM ammonium formate, +0.2% FA) as final spray solutions. The sample was introduced via direct infusion with a syringe pump using a flow-rate of 4 µL/min. Data were processed using DataAnalysis 5.2 (Bruker).

Molecular formulas of precursor and fragment masses were calculated in DataAnalysis using SmartFormula with a mass error of less than 0.5 ppm and a maximal formula of $C_xH_yN_2O_{20}P_2$. The molecular formulas of the precursor and fragments were confirmed by low mSigma values for good matching of the measured and calculated isotopic pattern.

Fermentation of *ape*$^+$ Strain. Four 20 L bioreactors (Braun; Melsungen) were filled with 20 L LB-medium supplemented with approx. 3 mL anti-foam (SILICON Antischaum US, C. Schliessmann, Schwäbisch Hall) each and sterilization (121°C, 40 min). After cooling down, they were inoculated with a preculture (1:100) of *ape*$^+$ (*X. doucetiae*Δ*DC*Δ*hfq*P$_{BAD}$*apeB*), supplemented with 0.2% L-arabinose (200 mL autoclaved 20% L-arabinose). The strain was cultivated for 72 h with 160 rpm at 30°C with 4 L compressed air/min. Cells were harvested with a flow-through centrifuge (Heraeus Contifuge Stratos equipped with a continuous flow rotor, Thermo Scientific) at 16 000 rpm. The cell culture was loaded with a flow-rate of 120-150 mL/min. The resulting cell pellet was freeze-dried and stored at -80°C for further experiments (extraction and isolation of APEL, see below).

Isolation of APELs-1284 (1), 1270 (2), 1256a (3) and 1242 (4) from *ape*$^+$. APELs were extracted in 22-44 g portions with 3 x 200 mL DCM:MeOH (2:1) from a total of 275 g freeze-dried cell pellets of *ape*$^+$ in 500 mL Shot-flasks. The extract was filtered into round flasks and evaporated

under reduced pressure to dryness. Per portion, 2-4 g crude extract was obtained. The resulting crude extract was resuspended in approx. 15 mL DCM/MeOH (2:1) and mixed with the same amount of silica gel. Again, the solvent was carefully evaporated under reduced pressure for dry-loading of a 100 g silica gel flash column (SNAP KP-Sil 100 g). Major impurities were eluted with 60-80 CV 50% PL-polar (50% chloroform) (for PL-polar and further specifications, see Table S6, 7 and 8). The yellow pigments were eluted with 15 CV of 75% PL-polar (25% chloroform). All yellow fractions were combined and evaporated to dryness, resulting in a ~2 g fraction containing APELs, which was again dry-loaded to a new 100 g silica gel column. The remaining impurities were eluted with 40 CV 50% PL-polar (50% chloroform), and APELs were eluted with a gradient of 50-85% PL-polar (50-15% chloroform) over 60 CV. Yellow fractions were monitored via TLC, the fractions with only minor amounts of impurities were combined and resulted in a total of 300 mg fraction mainly containing APELs (APEL Flash fraction; Fig. S5). An appropriate amount of sample, in total 150 mg, was repeatedly dissolved in DMF, and further subjected to semi-preparative HPLC-UV/MS with a reversed-phase/anionic exchange column (C18AX, Waters). The remaining sample was freeze-dried each time. The first reversed-phase isolation round resulted in 94 mg APEL-1284 (**1**), 45 mg APEL-1270 (**2**), 43 mg APEL-1256a (**3**), and 20 mg APEL-1242 (**4**). Due to impurities of accumulated Naugard stabilizer ($[M+H]^+$ 663.454)[7], probably derived from plastic containers of organic solvents, the compounds were subjected to a second round of reversed-phase purification, which resulted in 29 mg APEL-1284 (**1**), 18 mg APEL-1270 (**2**), 19 mg APEL-1256a (**3**), and 5 mg APEL-1242 (**4**). For detailed specifications of the purification procedure, see Table S6-8.

To avoid any unspecific products, light and oxygen were reduced to a minimum during the isolation process. Brown flasks or aluminum foil were used to cover the flasks/fractions.

Additionally, fractions obtained during the reversed-phase isolation process were freeze-dried only (Lyovapor L-300, BÜCHI, liquid nitrogen was used for freezing) and covered with nitrogen gas for storage at -80°C.

Additional information on the corresponding cultivation conditions and detailed purification conditions and further specifications are listed in Table S6-8.

NMR Spectroscopy. ^{1}H, ^{13}C, ^{31}P-decoupled ^{1}H, ^{1}H-decoupled ^{31}P, ^{1}H-^{13}C heteronuclear single quantum coherence (HSQC), ^{1}H-^{13}C/^{1}H-^{31}P heteronuclear multiple bond correlation (HMBC), ^{1}H-^{1}H double quantum filtered correlation spectroscopy (DQF-COSY), ^{1}H-^{13}C heteronuclear multiple quantum correlation/^{1}H-^{1}H correlation spectroscopy (HMQC-COSY), ^{1}H-^{13}C heteronuclear single quantum coherence/^{1}H-^{1}H total correlation spectroscopy (HSQC-TOCSY), ^{1}H-^{1}H Nuclear Overhauser Effect Spectroscopy (NOESY), and selective 1D ^{1}H-^{1}H TOCSY (O1P was set exactly at different excited resonances) were measured. Chemical shifts (δ) were reported in parts per million (ppm) and referenced to the DMF-d_7 solvent signals. Data are reported as follows: chemical shift, multiplicity (br = broad, s = singlet, d = doublet, t = triplet, m = multiplet, and ov = overlapped), and coupling constants in Hertz (Hz).

APEL-1242 (**4**), dissolved in 600 µL N,N-dimethylformamide (DMF)-d_7 (99.5%, Alfa Aesar), was measured in a 5 mm NMR tube. APELs-1284 (**1**), 1270 (**2**), and 1256a (**3**), dissolved in 160 µL DMF-d_7, were measured in 3 mm NMR tubes. To avoid possible degradation caused by light, we used brown NMR tubes or aluminum foil protection up until measurements. NMR experiments were acquired on Bruker Avance III HD 600 MHz (equipped with a 5 mm QCI cryoprobe), Bruker Avance III HD 800 MHz (equipped with a 5 mm TXO cryoprobe), Bruker Avance NEO 800 MHz (equipped with a 5 mm TCI cryoprobe), Bruker Avance III HD 900 MHz (equipped with a 5 mm TCI cryoprobe), and Bruker Avance III HD 950 MHz (equipped with a 5 mm TCI cryoprobe)

spectrometers. ^{1}H and ^{13}C NMR spectra were referenced to ^{1}H (δ_H 8.03) and ^{13}C (δ_C 163.2) chemical shifts of DMF-d_7 (internal reference). 85% phosphoric acid-d_3 (δ_P = 0 ppm) in D_2O was used as an external reference standard for ^{31}P NMR spectra. Bruker library standard NMR pulse sequences were employed for recording homo- and heteronuclear correlation NMR spectra. All the NMR spectra were processed using Bruker Topspin (Bruker BioSpin, Germany).

Detailed NMR Structural Elucidation of APEL-1270 (2). The structure and chemical shifts of APEL-1270 (**2**) were unambiguously assigned by using extensive 1D- and 2D-NMR spectra recorded in DMF-d_7 at 298 K. 1D-selective ^{1}H-^{1}H TOCSY spectrum of **2** irradiated at H-2 (δ_H 6.03, Fig. 2b, red) displays a coupled spin network of 12 protons indicates that **2** contains a polyene moiety with six conjugated double bonds. Out of 12 protons, H-2 and H-13 appeared as doublets with $^{3}J_{HH}$ couplings of 15.2 Hz and 15.5 Hz (*trans* over a double-bond), respectively, and the remaining ten protons (H-3 to H-12) appeared as a doublet of doublets with large $^{3}J_{HH}$ couplings of ~15 Hz (*trans* over a double-bond) and ~11 Hz (*trans* over a single-bond) revealed the *trans* configuration of all the double-bonds in the polyene chain (Table S10). The observed ^{1}H-^{13}C HMBC correlations of H-12/C-aromatic quaternary carbon and H-aromatic-ortho proton (δ_H 7.19 and 7.29)/C-13 (Fig. 2a) of **2** indicates the presence of an APE moiety with a 4-hydroxy-3-methylphenyl head group, identical to a previously characterized hydrolytic APE product from *E. coli* CFT073.[6] The structure of the aryl group was assigned based on the characteristic scalar coupling patterns of aromatic ortho- and meta-protons. Further, the oxymethylene protons (δ_H 4.32) displayed an HMBC correlation to the carbonyl center C-1 (δ_C 167.5) of APE, suggesting that the APE is linked to an *N*-acetylgalactosamine (GalNAc) moiety. The structure of GalNAc was further confirmed by the representative $^{3}J_{HH}$ (*axial-axial* and *axial-equatorial*) couplings, and

the strong NOE cross-peaks observed between H-22/H-23, H-24/H-25, H-25/H-26, and H-24/H-26 protons. A doublet at δ_H 8.8 ppm ($^3J_{H\text{-}23/NH}$ = 7.3 Hz) was assigned to an NH proton in the GalNAc and showed an HMBC correlation to the carbonyl ($\delta_{C\text{-}28}$ 172.6) of an acetyl group, confirming the presence of an N-acetyl group in the GalNAc moiety. However, the anomeric proton of GalNAc appeared as a doublet of doublets, which highlights the contribution of a long-range $^3J_{PH}$ coupling to the observed H-22 scalar coupling induced multiplet pattern. The doublet of doublets of H-22 was collapsed into a doublet in the ^{31}P-decoupled ^{1}H NMR spectrum, and a cross-peak between P-30 (δ_P -1.42) and H-22 observed in the 2D ^{1}H-^{31}P HMBC spectrum strongly support the above interpretation that a phosphate group is linked to the GalNAc at the anomeric carbon (-C-O-P- bond). Thus, a phosphate connected to the APE moiety via a GalNAc in an α-1,6 linkage is established. Further, the glycerol moiety bonded (-C-O-P- linkage) to the phosphate group was assigned based on the HMBC cross-peaks between P-30 and methylene protons (H-31, δ_H 4.09, 3.99) and the corresponding spectral changes observed in the ^{31}P-decoupled ^{1}H NMR spectrum of **2**. The glycerol 2-acyl chain was assigned based on the HMBC correlation of H-32, H-35, and H-36 protons to the carbonyl carbon (δ_C 171.7) of an ester group. 1D-selective ^{1}H-^{1}H TOCSY spectrum of **2** irradiated at H-37 (δ_H 5.84, Fig. 2b, green) in combination with the 2D ^{1}H-^{1}H DQF-COSY spectrum highlights that the glycerol 2-acyl chain (C26) contains 5 conjugated double bonds. Subsequently, the configuration around each of the 5 double bonds was confirmed as *trans* based on the large $^3J_{HH}$ couplings (~15 Hz) observed between the olefinic protons. The methylene protons H-61 and H-33 showed an HMBC correlation to the carbonyl center (δ_C 174.0) of an ester group establishing the linkage between the glycerol backbone and the 3-acyl chain. Afterward, the C16 fully saturated fatty acyl chain was confirmed by the 2D HSQC-TOCSY and HMQC-COSY NMR spectra analysis, which was further supported by the MS/MS fragmentation

analysis. The stereochemistries of C-32 and C-36 and the absolute configuration of the GalNAc moiety have not been determined yet.

Phylogeny. A set of over 20,000 bacterial genomes from the antiSMASH database 2.0[8] was used to survey the presence of *ape* BGCs across known bacterial isolates. This set represents redundancy and quality filtered genomes from the NCBI Refseq database to ensure maximum completeness for each genome. Phylogenetic inference was performed using 16S sequences extracted from each genome that showed at least 1000 bp of length. Alignments were generated with MAFFT followed by tree inference using Fasttree.[9,10] *ape* BGCs were marked as "arypolyene" by antiSMASH[8] were used to annotated presence and absence on the phylogenetic tree. The presence of core genes was detected using the following antiSMASH and Pfam[11] models for each gene: KS/CLF (APE_KS1/2), ACP (PF00550.21), DH (PF07977.9), KR (PF08659.6), and MMPL transporter (PF03176.11). These were searched using HMMER[12] v3 with trusted cut-off enabled. All annotations, including NCBI taxonomy designations, were visualized using the iTOL server.[13] Further details, such as branch lengths and genus designations, can be explored online: https://itol.embl.de/tree/21312710124131044160103833 9.

Supplementary Figures

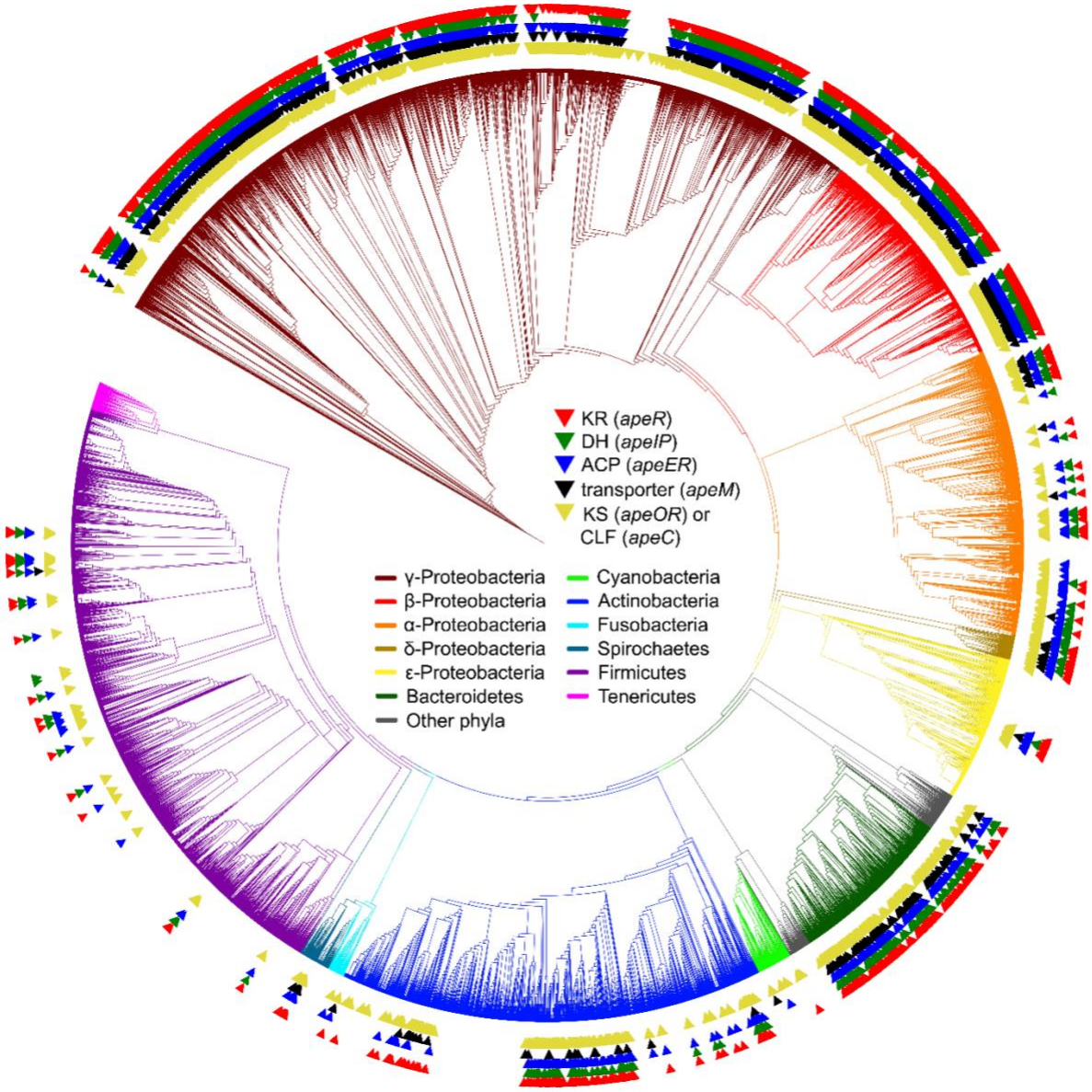

Fig. S1. Distribution of putative *ape* BGCs detected by the occurrence of different core genes across a phylogenetic tree of 16S rRNA sequences extracted from the antiSMASH database. Triangles depict the presence of putative *ape* BGCs detected by KS/CLF (Pfam 13723, yellow), ACP (Pfam 00550, blue), DH (Pfam 07977, green), KR (Pfam 08659, red), or MMPL transporter (Pfam 03176, black). Yellow triangles show the presence of KS or CLF proteins that are detected with APE models in antiSMASH. NCBI taxonomy designations are shown as clade colors.

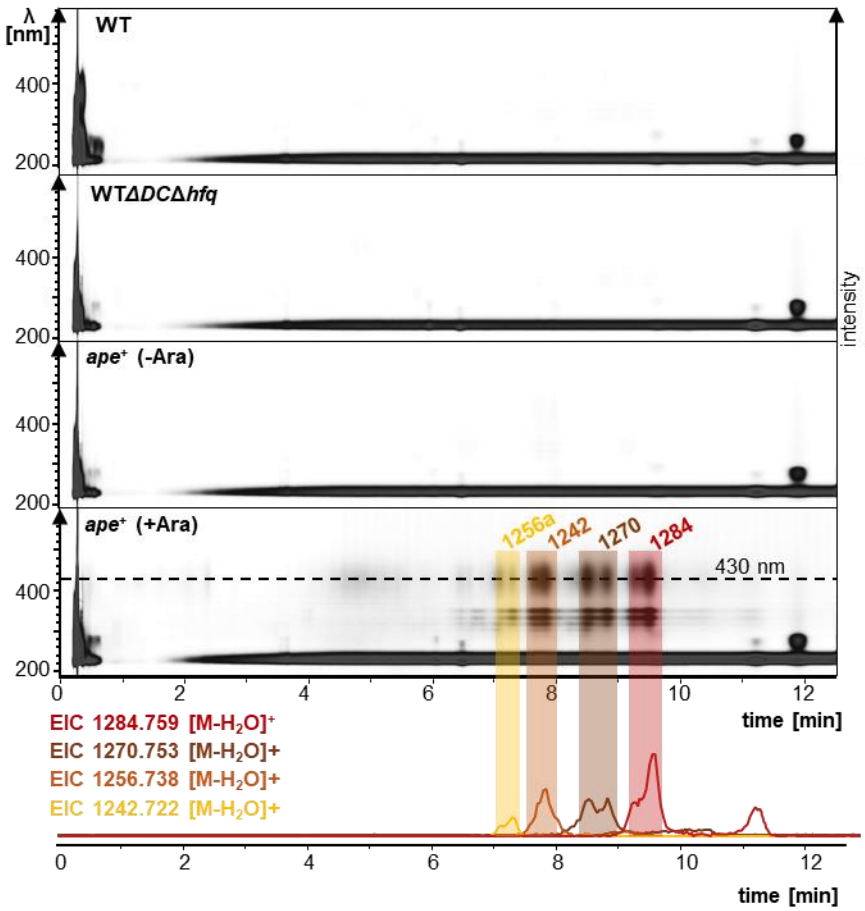

Fig. S2. HPLC-UV/MS analysis of the *X. doucetiae* mutants in comparison to its cognate wildtype strain. Displayed are the survey views of the *X. doucetiae* DSM 17909 wildtype (WT), the secondary metabolite deficient strain *X. doucetiae* DSM 17909Δ*DC*Δ*hfq* (WTΔ*DC*Δ*hfq*)[14] and the corresponding mutant, carrying an arabinose inducible promoter in front of the *ape* BGC (*X. doucetiae* DSM 17909 Δ*DC*Δ*hfq*P_{BAD}*apeB*, *ape*$^+$)[15] with (+Ara) and without arabinose induction (-Ara). Depicted in the bottom are the EICs (±0.005 Da) of the major APELs 1242 (**4**), 1256a (**3**), 1270 (**2**), and 1284 (**1**). The split UV/EIC profiles might be due to a special chromatographic behavior of APE containing compounds.

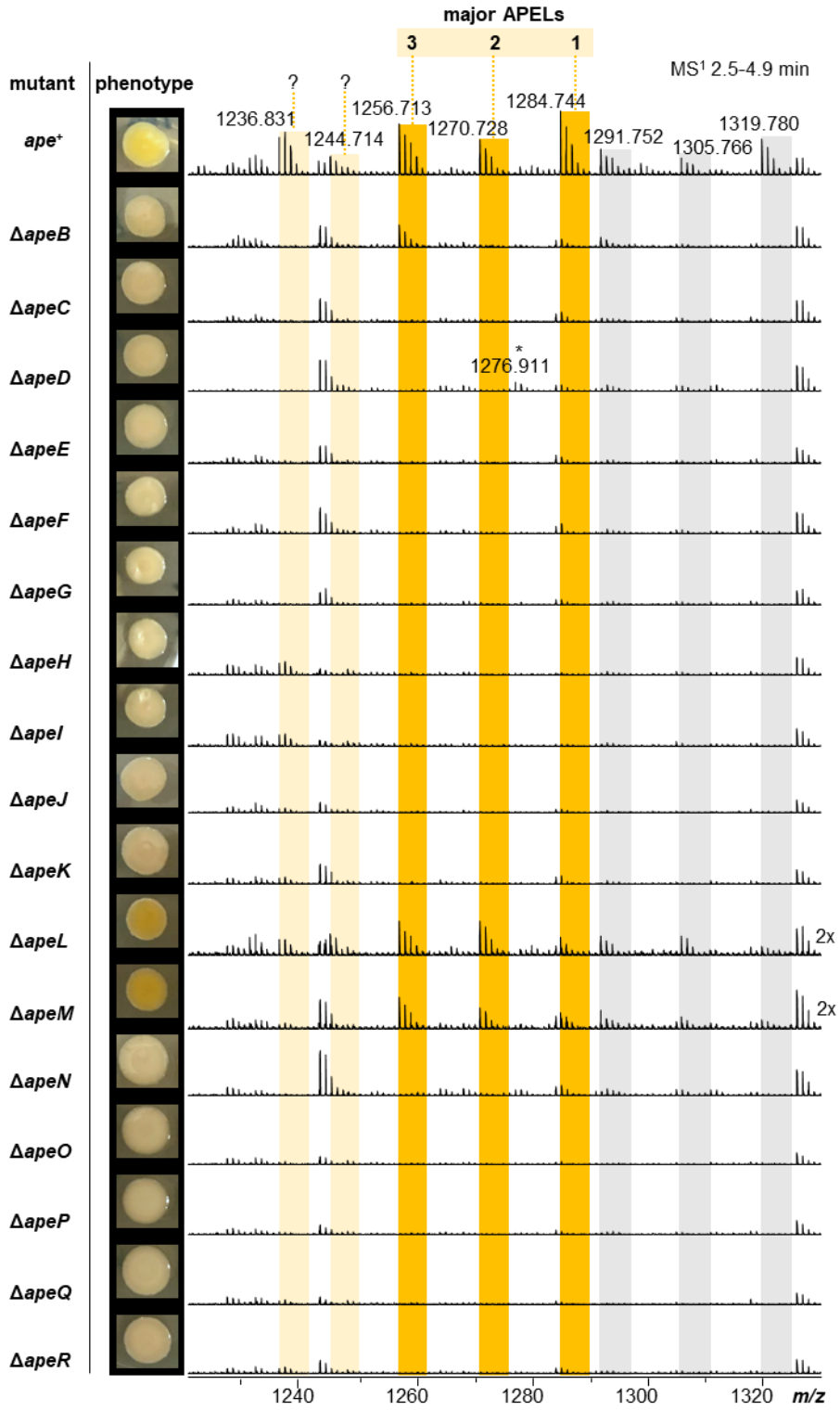

Fig. S3. MS detection of APELs in the *ape*$^+$ strain and corresponding single *ape* gene deletion mutants Δ*apeB-R*. Summarized HPLC/MS^1 analysis of all strains from 2.5-4.9 min with the corresponding phenotype on LB agar plates (left). MS signals of the major APELs, APEL-1284 (**1**), APEL-1270 (**2**), and APEL-1256a (**3**), are highlighted in dark yellow. MS signals of additional but uncharacterized APEL derivatives are shown in light yellow. A uncharacterized signal present in the Δ*apeD* mutant is indicated by an asterisk. Other MS adducts of APELs are indicated by grey shapes (see also Figure S12). A comparison of the corresponding survey view data is shown in Figure S4.

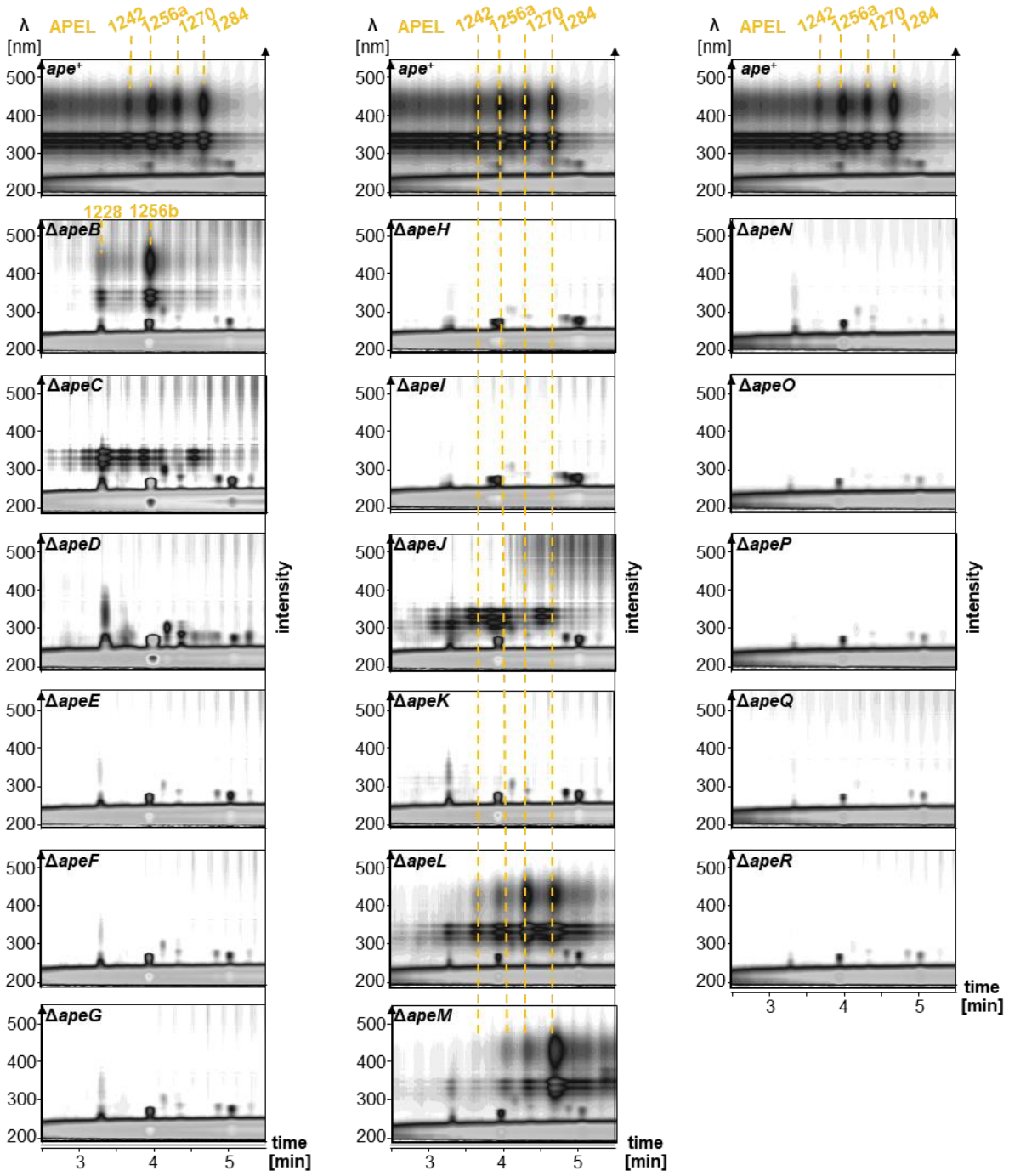

Fig. S4. HPLC-UV/MS analysis in survey view of the *ape*$^{+}$ strain compared to the *ape*$^{+}$ mutant strains with deletions of *apeB-R*, with annotations for APELs-1284 (**1**), 1270 (**2**), 1256a (**3**), 1242 (**4**), 1256b (**5**), and 1228 (**6**).

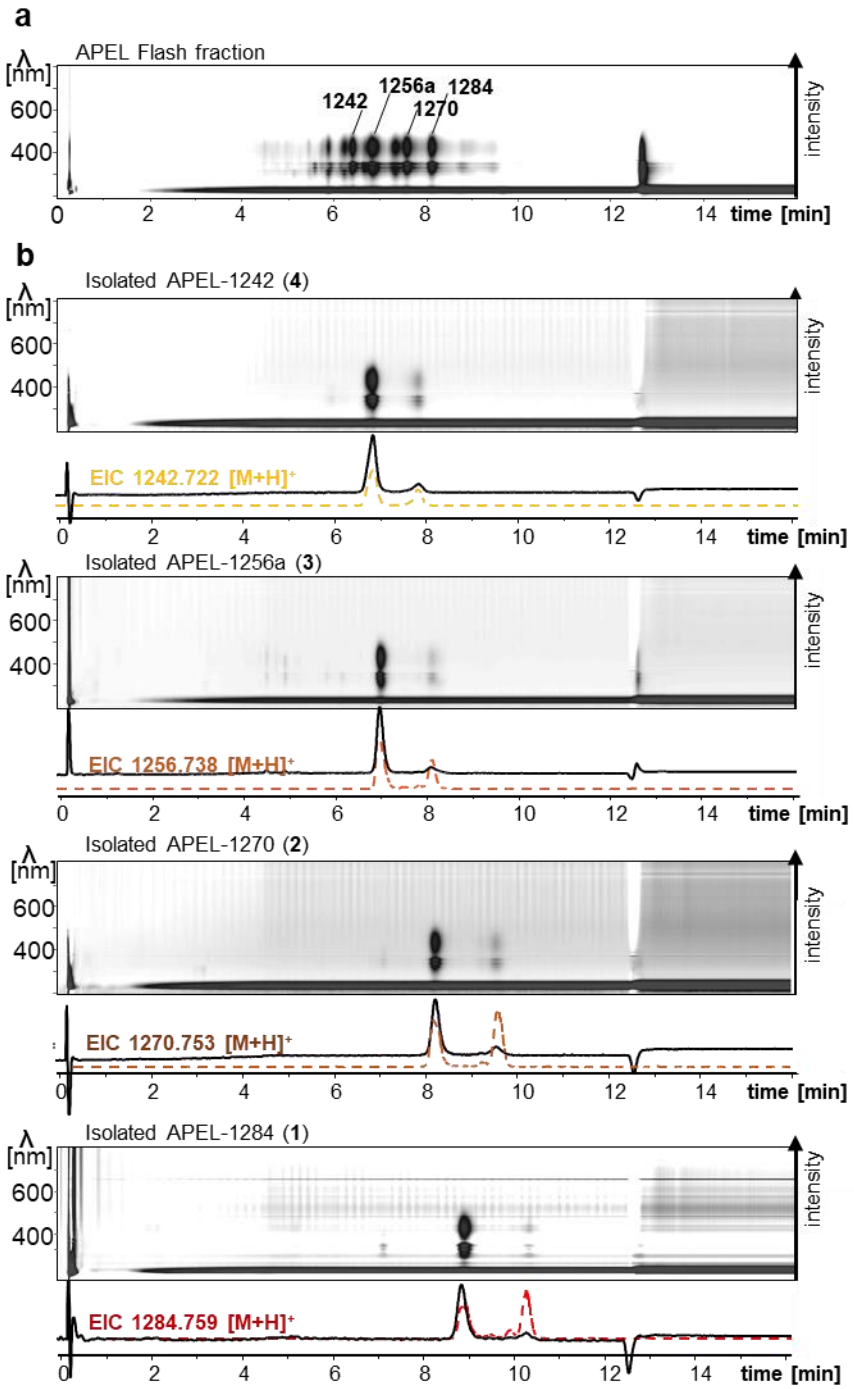

Fig. S5. HPLC-UV/MS profiles of (**a**) a fraction mainly containing APELs obtained by flash silica gel chromatography, in comparison with (**b**) pure APELs-1284 (**1**), 1270 (**2**), 1256a (**3**), and 1242 (**4**). Shown are survey views, UV profiles (detection wavelength 430 nm, solid line), and EICs (dotted lines).

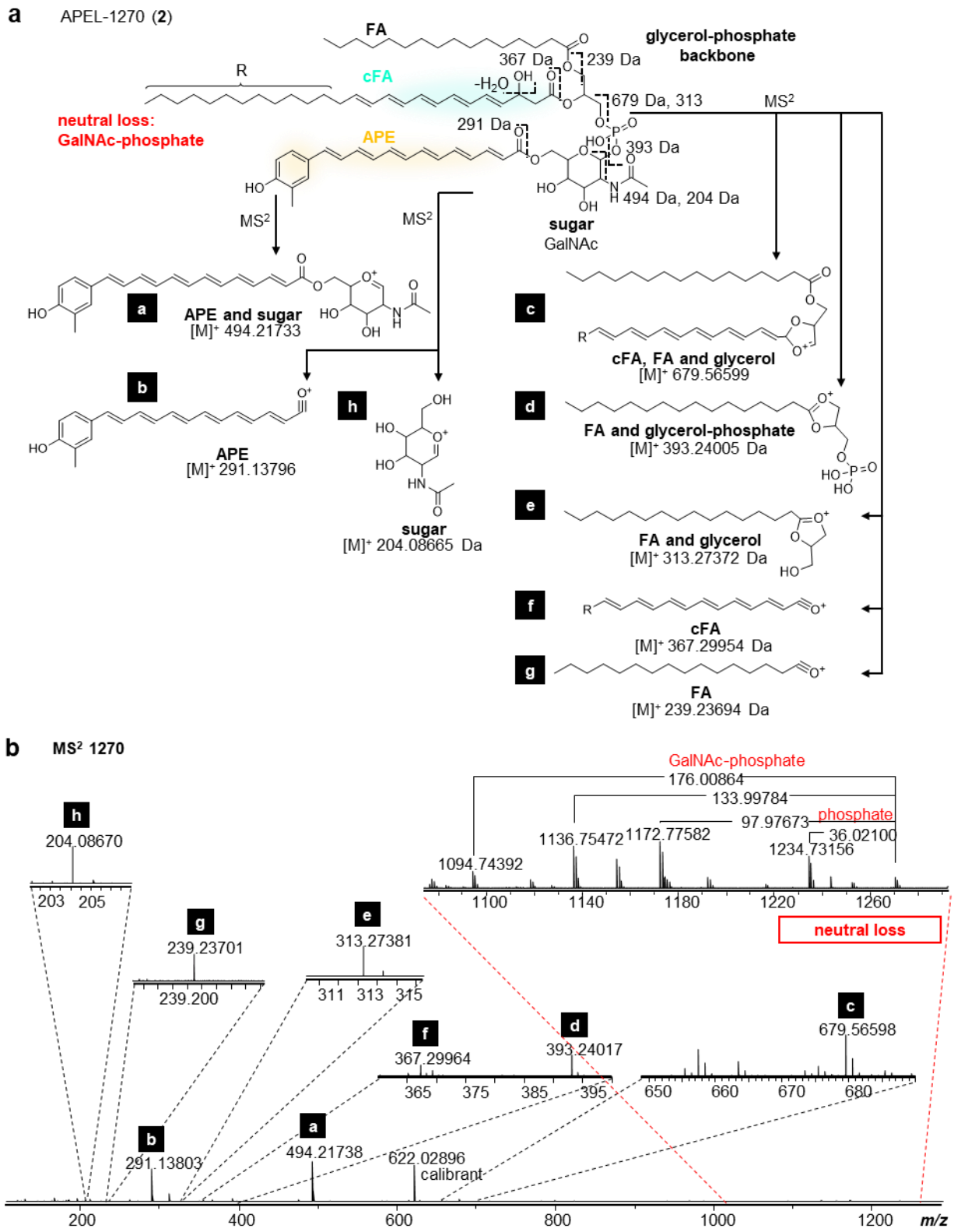

Fig. S6. Diagnostic MS/MS fragmentation of APEL-1270 (**2**). Collision induced fragment ions are shown schematically (**a**) with annotations and expansions on the spectrum (**b**).

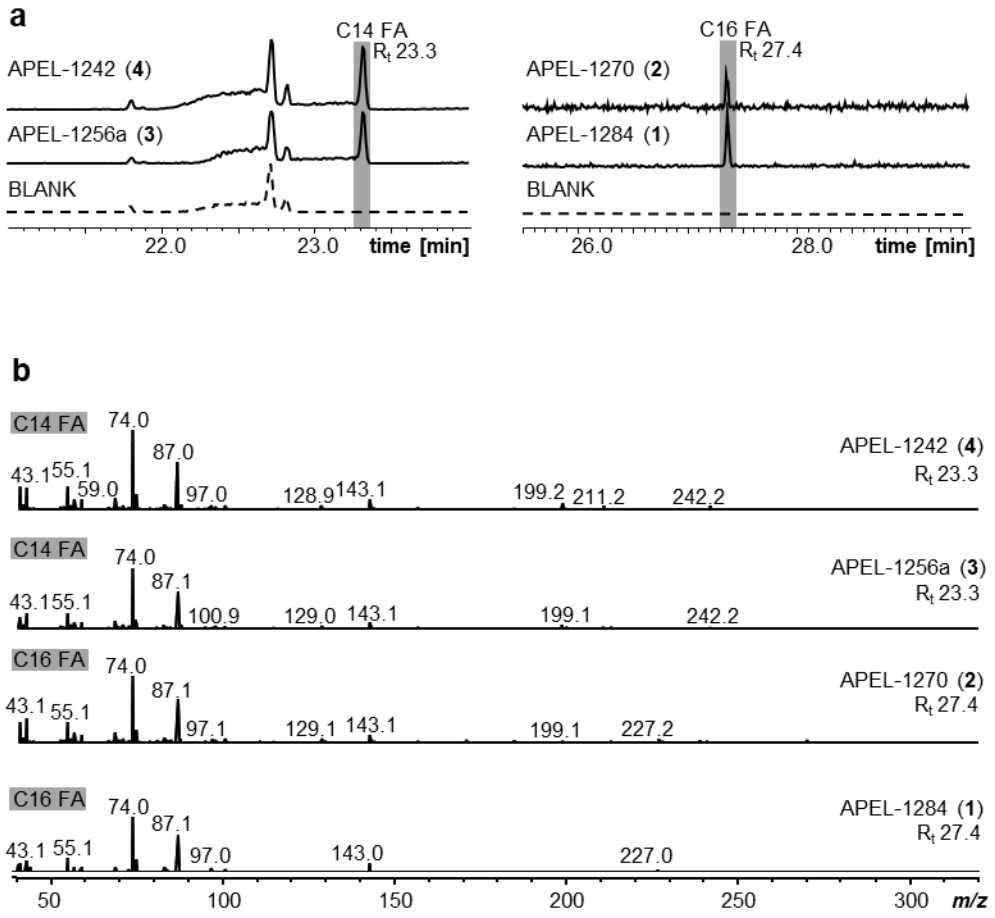

Fig. S7. GC-MS analysis of the fully saturated fatty acyl chains in pure APELs. (**a**) GC-chromatograms of FAMEs derived pure APELs. (**b**) MS fragmentation patterns of FAMEs derived fatty acids.

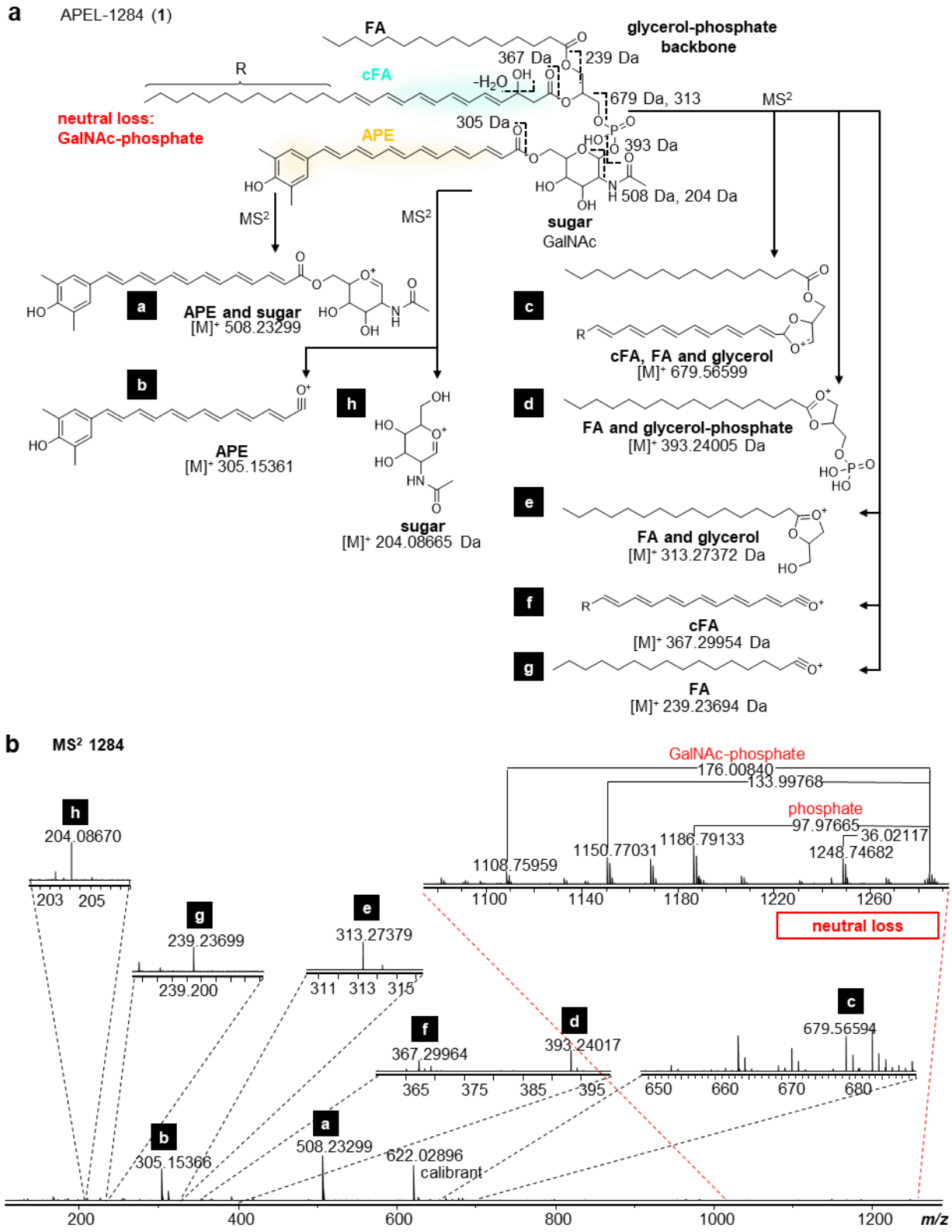

Fig. S8. Diagnostic MS/MS fragmentation of APEL-1284 (**1**). Collision induced fragment ions are shown schematically (**a**) with annotations and expansions on the spectrum (**b**).

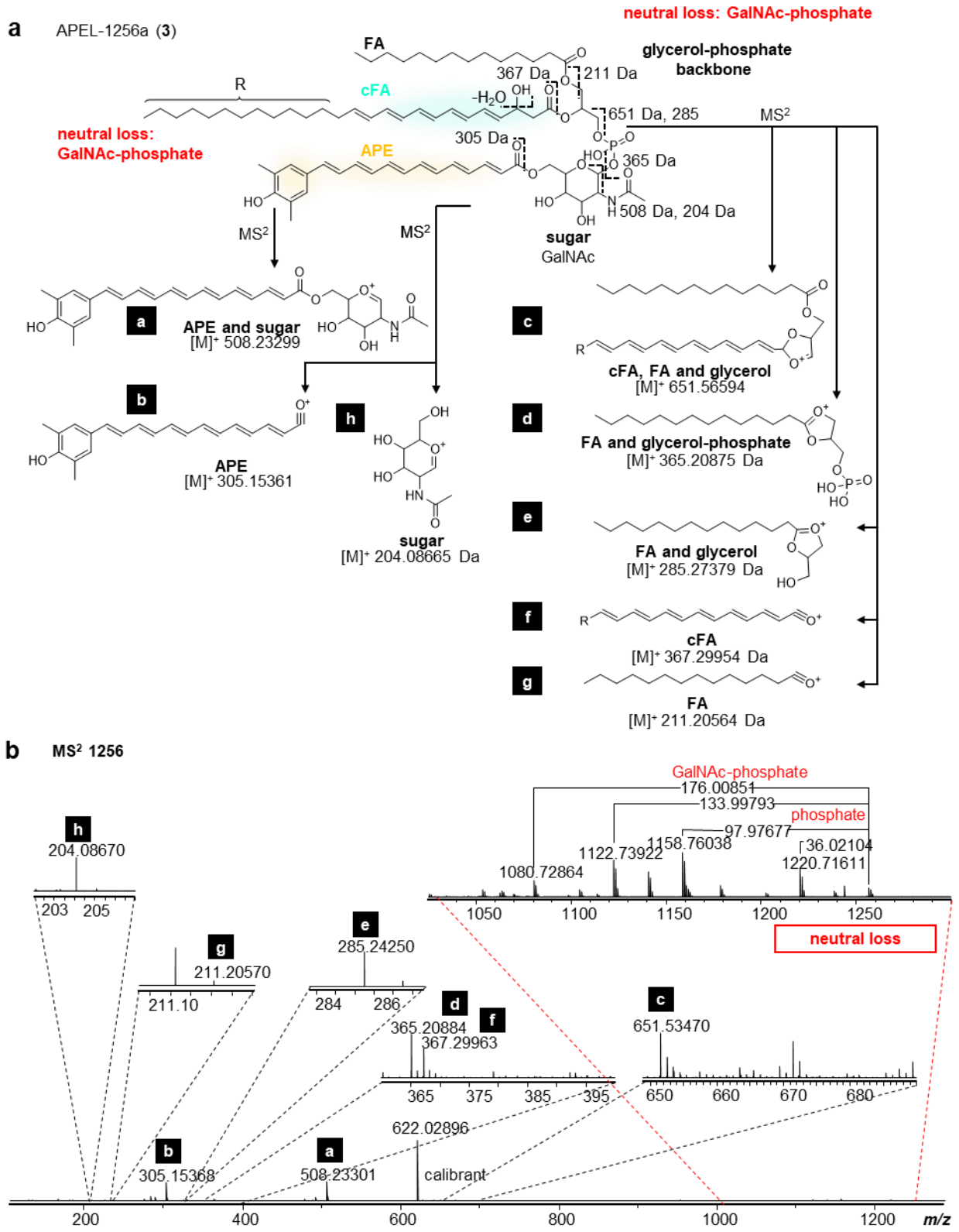

Fig. S9. Diagnostic MS/MS fragmentation of APEL-1256a (**3**). Collision induced fragment ions are shown schematically (**a**) with annotations and expansions on the spectrum (**b**).

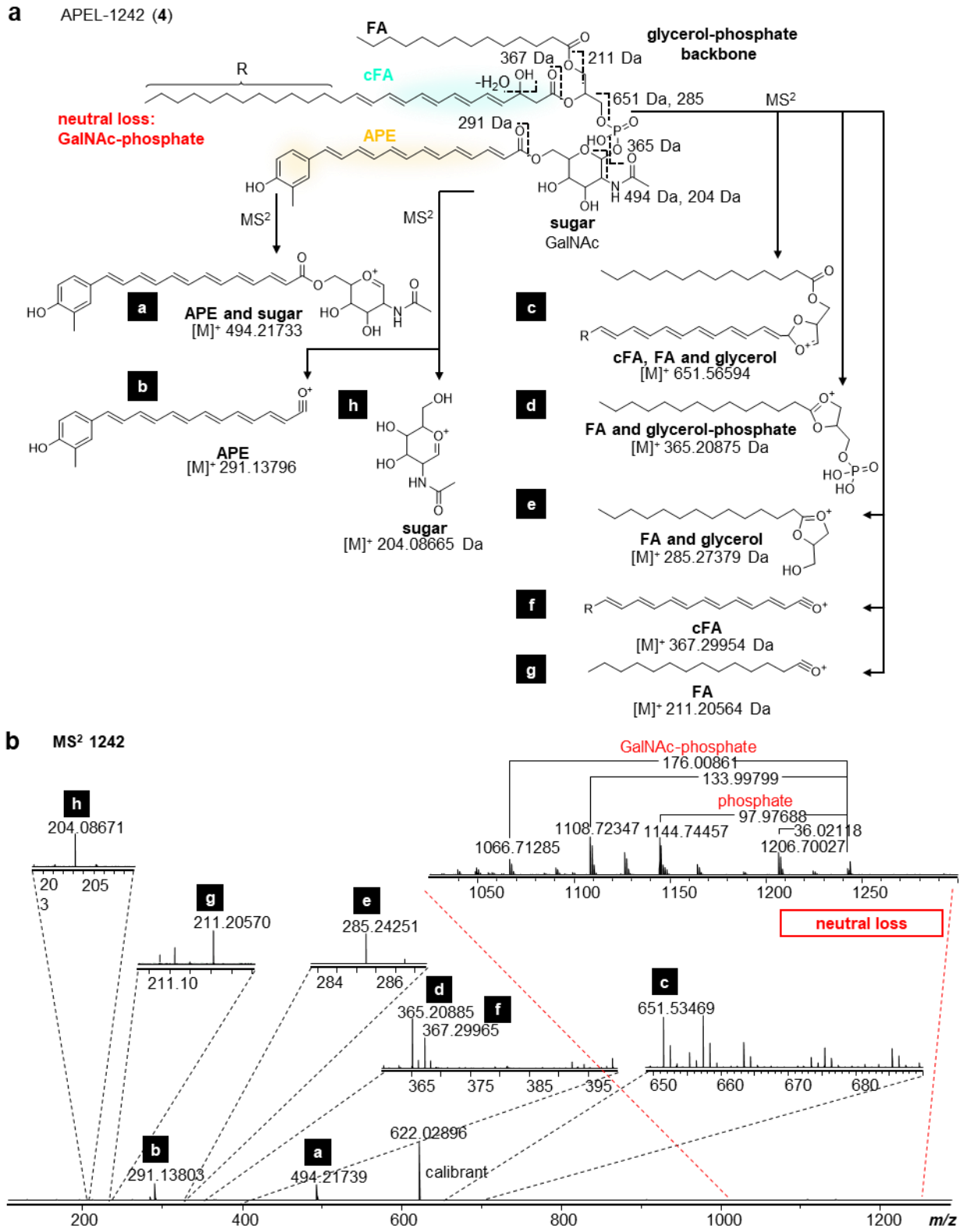

Fig. S10. Diagnostic MS/MS fragmentation of APEL-1242 (**4**). Collision induced fragment ions are shown schematically (**a**) with annotations and expansions on the spectrum (**b**).

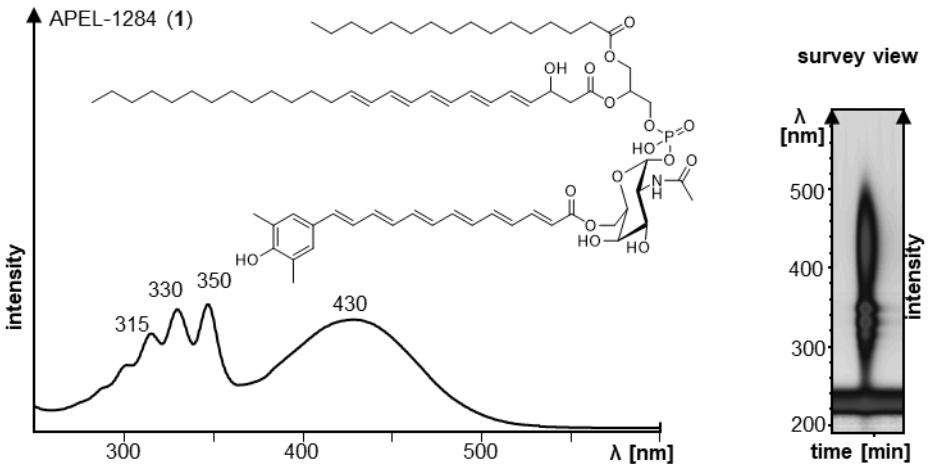

Fig. S11. Diagnostic UV absorption (250-600 nm) of APELs, exemplified by APEL-1284 (**1**) with its survey view (right).

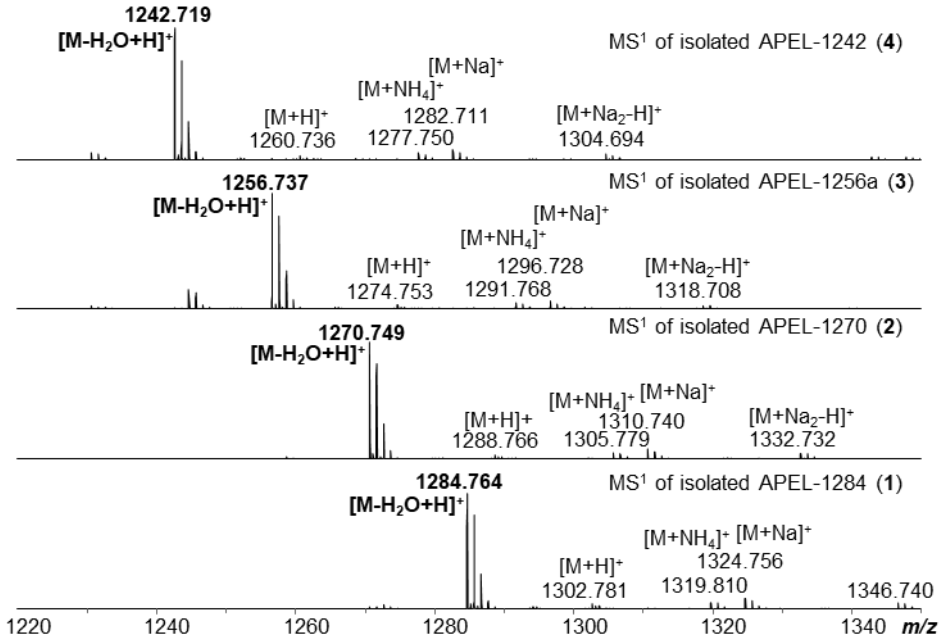

Fig. S12. Pseudo-molecular ions of APELs (**1-4**), see also Table S9.

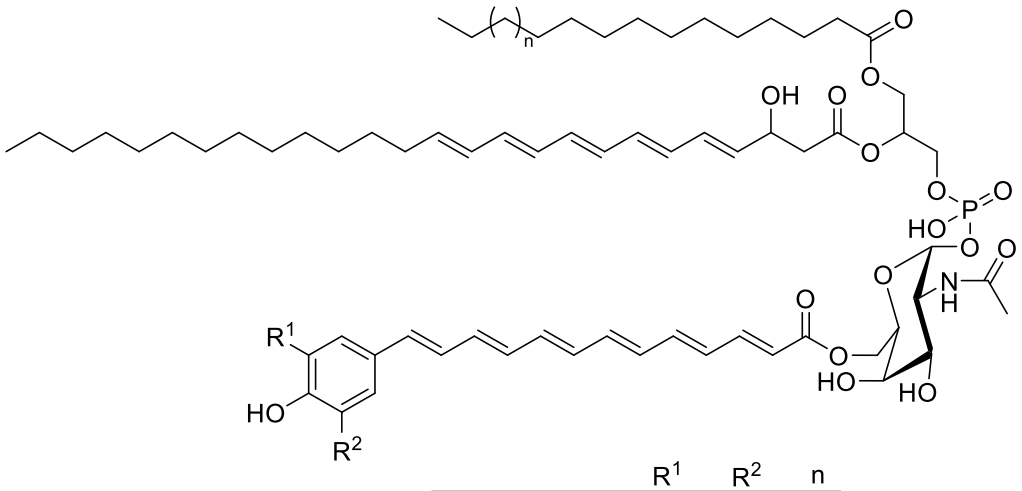

	R^1	R^2	n
APEL-1284 (**1**)	CH_3	CH_3	3
APEL-1270 (**2**)	CH_3	H	3
APEL-1256a (**3**)	CH_3	CH_3	1
APEL-1242 (**4**)	CH_3	H	1
APEL-1256b (**5**)	H	H	3
APEL-1228 (**6**)	H	H	1

Fig. S13. Chemical structures of APELs that were identified in this work.

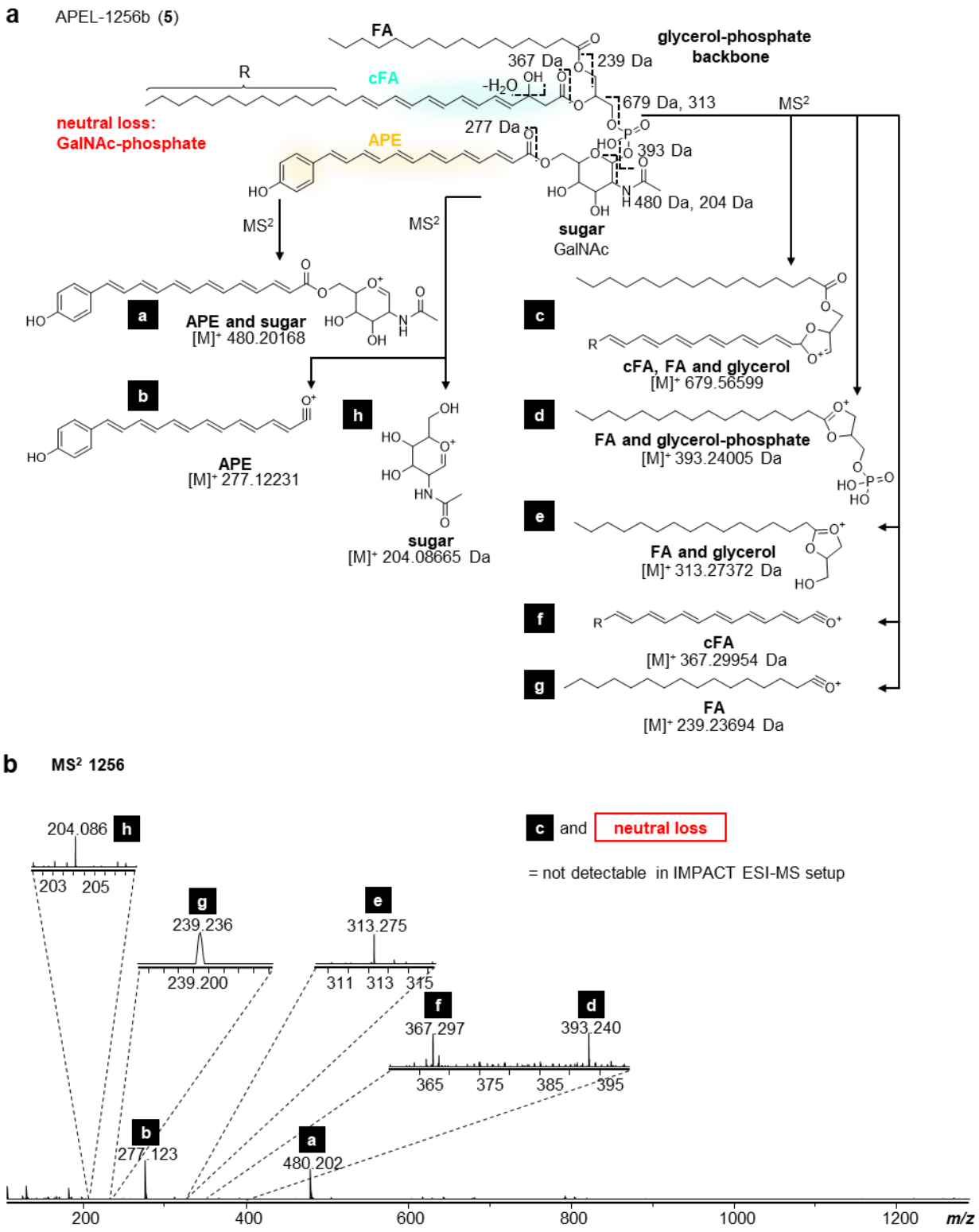

Fig. S14. Diagnostic MS/MS fragmentation of APEL-1256b (**5**). Collision induced fragment ions are shown schematically (**a**) with annotations and expansions on the spectrum (**b**).

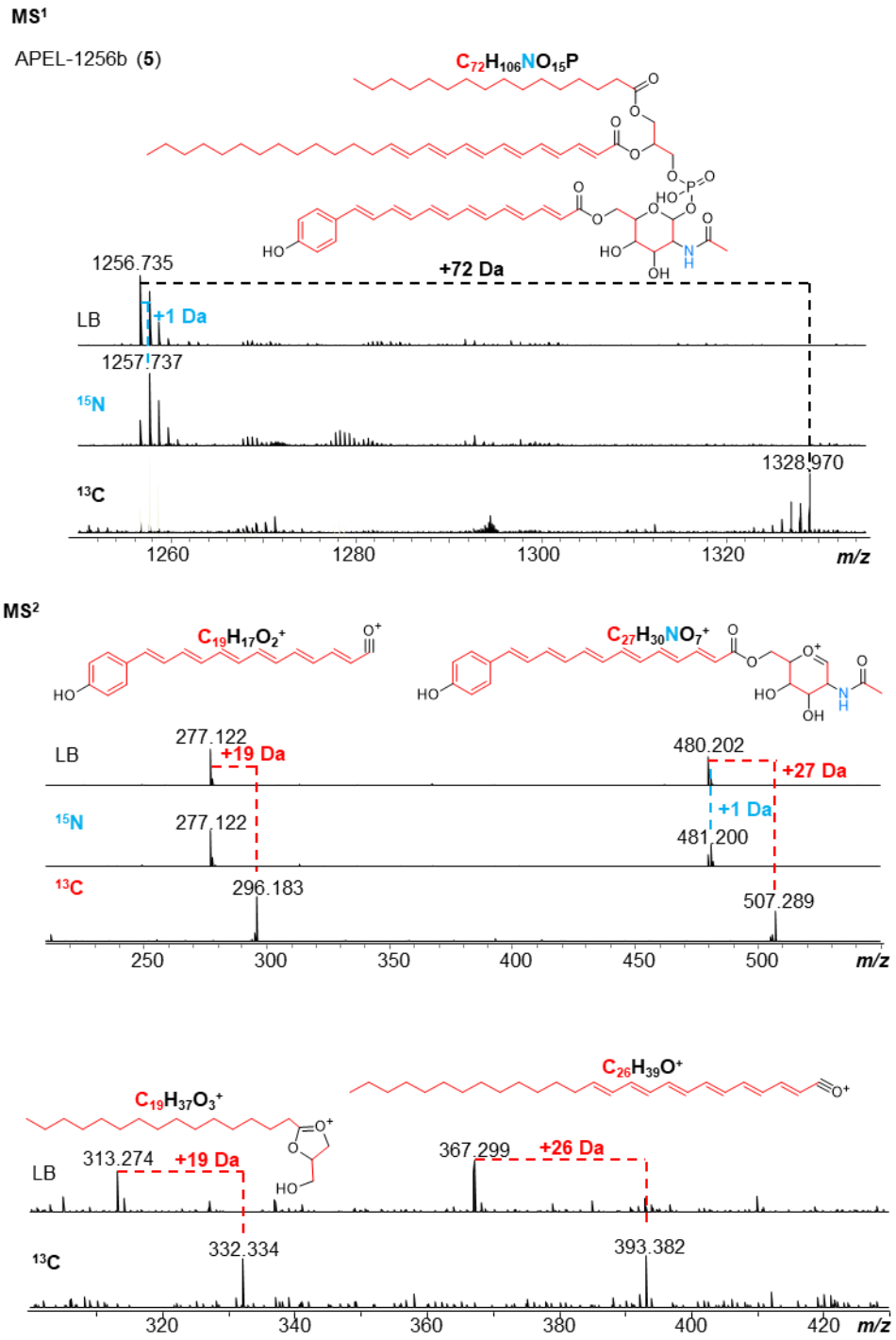

Fig. S15. ^{15}N and ^{13}C labeling experiments, exemplified by APEL-1256b (**5**) from the *ape*$^{+}$ mutant *ΔapeB*. Depicted are the mass shifts (dash lines) of the parent masses in MS^{1} and four characteristic fragments in MS^{2}. Dashed lines indicate mass shifts resulting from incorporation of nitrogen (blue) and carbons (red).

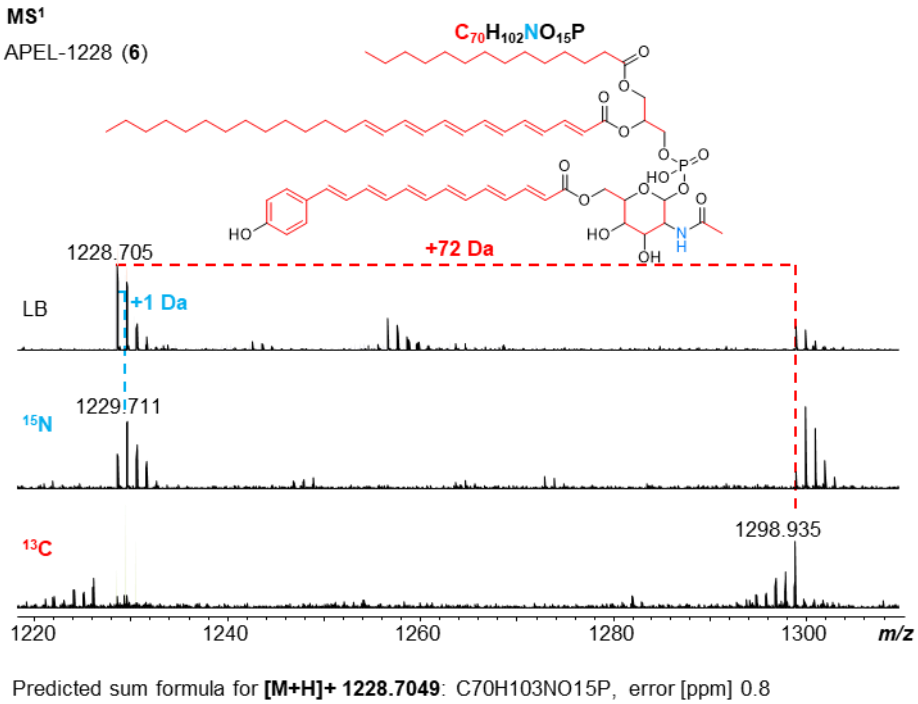

Fig. S16. ^{15}N and ^{13}C labeling experiments of APEL-1228 (**6**) from the *ape*$^{+}$ mutant *ΔapeB*. Depicted are the mass shifts (dash lines) of the parent masses in MS^1. Dashed lines indicate mass shifts resulting from incorporation of nitrogen (blue) and carbons (red).

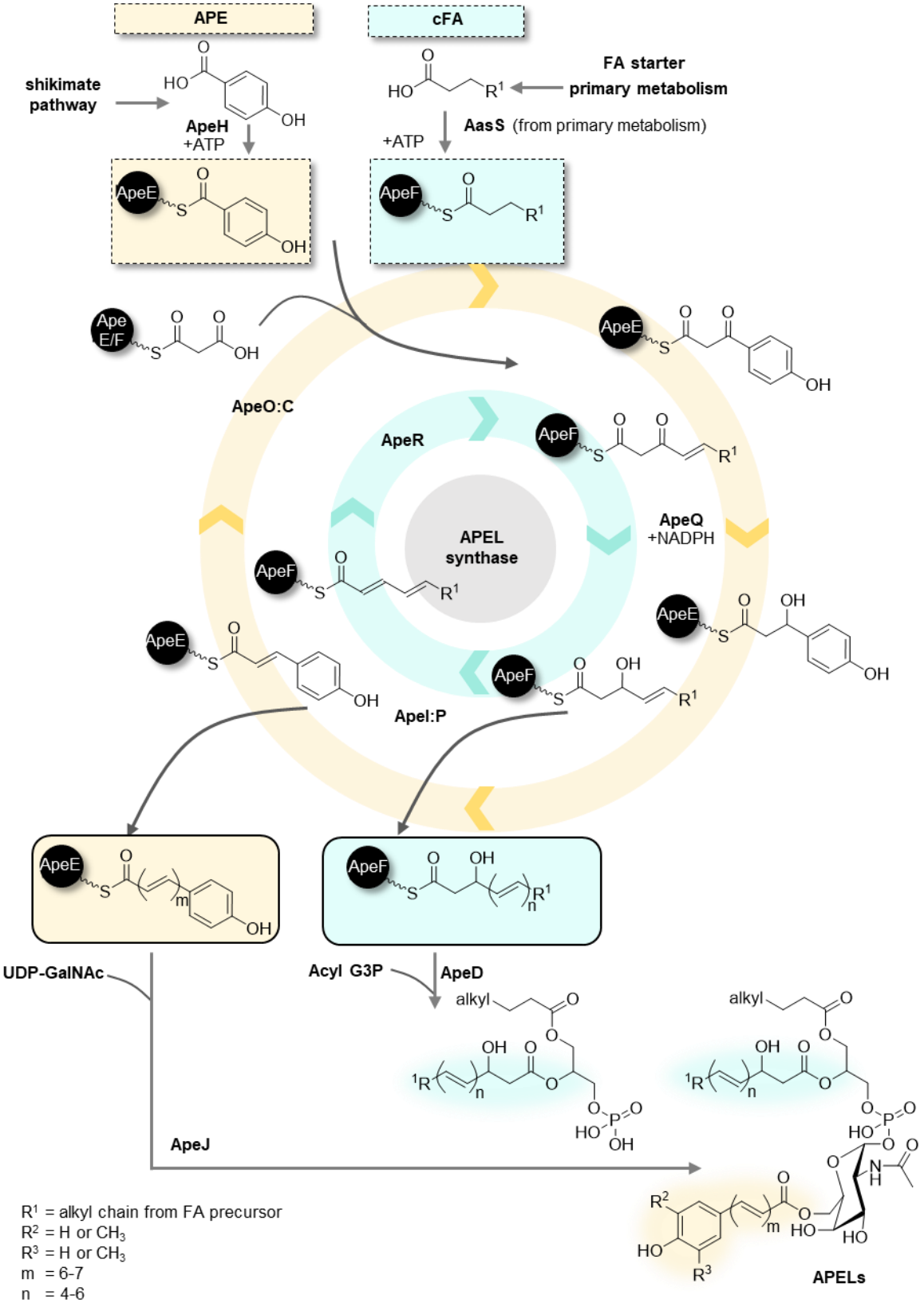
APE
cFA
shikimate pathway
ApeH +ATP
FA starter
primary metabolism
AasS (from primary metabolism)
+ATP
ApeE
ApeF
Ape E/F
ApeO:C
ApeR
ApeQ +NADPH
APEL synthase
Apel:P
UDP-GalNAc
Acyl G3P
ApeD
ApeJ
APELs
R¹ = alkyl chain from FA precursor
R² = H or CH₃
R³ = H or CH₃
m = 6-7
n = 4-6

Fig. S17. Proposed biosynthesis of APELs. The biosynthesis-route for the APE part is highlighted in yellow, and the conjugated FA (cFA) in turquoise. The precursors derived from primary metabolism are adenylated (+ATP) and both acyl moieties are transferred to the corresponding ACP through the action of AasS enzymes (ApeH for 4-hydroxy benzoic acid and AasS from primary metabolism for FA precursor). Elongation takes place with either ApeO:C (APE part) or ApeR (cFA part) in a decarboxylative Claisen-condensation reaction with malonate units, to result in the respective β-ketoacyl-ACP, which gets further reduced (ApeQ, NADPH) and dehydrated (DH complex ApeI:P). This cycle is sequentially repeated to result in the full-length APE-ACP (ApeE) and cFA-ACP (ApeF). The cFA is transferred to an acyl-glycerol-3-phosphate (acyl-G3P) by the G3P AT ApeD. The resulting G3P-double acylated intermediate is further glycosylated with *N*-acetyl-galactosamine (GalNAc) and acylated with the ACP-bound APE moiety, both of which with the help of the bifunctional glycosyl/acyltransferase ApeJ. Methylation of the aryl by ApeB is not displayed but is proposed to occur *in situ*.

Supplementary Tables

Table S1. Strains used in this study.

Strain	Genotype	Reference
E. coli ST18-λpir	Tp^r Sm^r, *recA thi hsdR*$^+$ RP4-2-Tc::Mu-Km::Tn7, *λpir* phage lysogen, Δ*hemA*	[16]
X. doucetiae DSM 17909^T	Wild type, amp^r	DSMZ
X. doucetiae DSM 17909^{T}Δ*DC*Δ*hfq* (WTΔ*DC*Δ*hfq*)	*X. doucetiae* DSM 17909^T wild type with a deletion in XDD1_RS09835 (decarboxylase) and *hfq*; amp^r,	[14]
X. doucetiae DSM 17909^{T}Δ*DC*Δ*hfq* P_{BAD}*apeB* (*ape*$^+$)	*X. doucetiae* DSM 17909^{T}Δ*DC*Δ*hfq* with a markerless promoter exchange in front of *apeB*, amp^r,	[15]
X. doucetiae DSM 17909^{T}Δ*DC*Δ*hfq* P_{BAD}*apeB*Δ*apeB* (*ape*$^+$Δ*apeB*)	*X. doucetiae* DSM 17909^{T}Δ*DC*Δ*hfq* with a markerless promoter exchange in front of *apeB* and with a deletion of *apeB*, amp^r	this work
X. doucetiae DSM 17909^{T}Δ*DC*Δ*hfq* P_{BAD}*apeB*Δ*apeC* (*ape*$^+$Δ*apeC*)	*X. doucetiae* DSM 17909^{T}Δ*DC*Δ*hfq* with a markerless promoter exchange in front of *apeB* and with a deletion of *apeC*, amp^r	this work
X. doucetiae DSM 17909^{T}Δ*DC*Δ*hfq* P_{BAD}*apeB*Δ*apeD* (*ape*$^+$Δ*apeD*)	*X. doucetiae* DSM 17909^{T}Δ*DC*Δ*hfq* with a markerless promoter exchange in front of *apeB* and with a deletion of *apeD*, amp^r	this work
X. doucetiae DSM 17909^{T}Δ*DC*Δ*hfq* P_{BAD}*apeB*Δ*apeE* (*ape*$^+$Δ*apeE*)	*X. doucetiae* DSM 17909^{T}Δ*DC*Δ*hfq* with a markerless promoter exchange in front of *apeB* and with a deletion of *apeE*, amp^r	this work
X. doucetiae DSM 17909^{T}Δ*DC*Δ*hfq* P_{BAD}*apeB*Δ*apeF* (*ape*$^+$Δ*apeF*)	*X. doucetiae* DSM 17909^{T}Δ*DC*Δ*hfq* with a markerless promoter exchange in front of *apeB* and with a deletion of *apeF*, amp^r	this work
X. doucetiae DSM 17909^{T}Δ*DC*Δ*hfq* P_{BAD}*apeB*Δ*apeG* (*ape*$^+$Δ*apeG*)	*X. doucetiae* DSM 17909^{T}Δ*DC*Δ*hfq* with a markerless promoter exchange in front of *apeB* and with a deletion of *apeG*, amp^r	this work
X. doucetiae DSM 17909^{T}Δ*DC*Δ*hfq* P_{BAD}*apeB*Δ*apeH* (*ape*$^+$Δ*apeH*)	*X. doucetiae* DSM 17909^{T}Δ*DC*Δ*hfq* with a markerless promoter exchange in front of *apeB* and with a deletion of *apeH*, amp^r	this work
X. doucetiae DSM 17909^{T}Δ*DC*Δ*hfq* P_{BAD}*apeB*Δ*apeI* (*ape*$^+$Δ*apeI*)	*X. doucetiae* DSM 17909^{T}Δ*DC*Δ*hfq* with a markerless promoter exchange in front of *apeB* and with a deletion of *apeI*, amp^r	this work
X. doucetiae DSM 17909^{T}Δ*DC*Δ*hfq* P_{BAD}*apeB*Δ*apeJ* (*ape*$^+$Δ*apeJ*)	*X. doucetiae* DSM 17909^{T}Δ*DC*Δ*hfq* with a markerless promoter exchange in front of *apeB* and with a deletion of *apeJ*, amp^r	this work
X. doucetiae DSM 17909^{T}Δ*DC*Δ*hfq* P_{BAD}*apeB*Δ*apeK* (*ape*$^+$Δ*apeK*)	*X. doucetiae* DSM 17909^{T}Δ*DC*Δ*hfq* with a markerless promoter exchange in front of *apeB* and with a deletion of *apeK*, amp^r	this work
X. doucetiae DSM 17909^{T}Δ*DC*Δ*hfq* P_{BAD}*apeB*Δ*apeL* (*ape*$^+$Δ*apeL*)	*X. doucetiae* DSM 17909^{T}Δ*DC*Δ*hfq* with a markerless promoter exchange in front of *apeB* and with a deletion of *apeL*, amp^r	this work
X. doucetiae DSM 17909^{T}Δ*DC*Δ*hfq* P_{BAD}*apeB*Δ*apeM* (*ape*$^+$Δ*apeM*)	*X. doucetiae* DSM 17909^{T}Δ*DC*Δ*hfq* with a markerless promoter exchange in front of *apeB* and with a deletion of *apeM*, amp^r	this work
X. doucetiae DSM 17909^{T}Δ*DC*Δ*hfq* P_{BAD}*apeB*Δ*apeN* (*ape*$^+$Δ*apeN*)	*X. doucetiae* DSM 17909^{T}Δ*DC*Δ*hfq* with a markerless promoter exchange in front of *apeB* and with a deletion of *apeN*, amp^r	this work

X. doucetiae DSM 17909^{T}Δ*DC*Δ*hfq* P_{BAD}*apeBΔapeO* (*ape*$^{+}$Δ*apeO*)	*X. doucetiae* DSM 17909^{T}Δ*DC*Δ*hfq* with a markerless promoter exchange in front of *apeB* and with a deletion of *apeO*, amp^{r}	this work
X. doucetiae DSM 17909^{T}Δ*DC*Δ*hfq* P_{BAD}*apeBΔapeP* (*ape*$^{+}$Δ*apeP*)	*X. doucetiae* DSM 17909^{T}Δ*DC*Δ*hfq* with a markerless promoter exchange in front of *apeB* and with a deletion of *apeR* and with a deletion of *apeP*, amp^{r}	this work
X. doucetiae DSM 17909^{T}Δ*DC*Δ*hfq* P_{BAD}*apeBΔapeQ* (*ape*$^{+}$Δ*apeQ*)	*X. doucetiae* DSM 17909^{T}Δ*DC*Δ*hfq* with a markerless promoter exchange in front of *apeB* and with a deletion of *apeQ*, amp^{r}	this work
X. doucetiae DSM 17909^{T}Δ*DC*Δ*hfq* P_{BAD}*apeBΔapeR* (*ape*$^{+}$Δ*apeR*)	*X. doucetiae* DSM 17909^{T}Δ*DC*Δ*hfq* with a markerless promoter exchange in front of *apeB* and with a deletion of *apeR*, amp^{r}	this work

Table S2. Oligonucleotides used in this study.

Plasmid/PCR	Oligonucleotide 5` to 3`		Template
Plasmid backbone	GG23	GAGCTCTCCCGGGAATTCC	pEB17
	GG138	AGGATCGATCCTTTTTAACCCATC	
pEB17Δ*apeB*	GG143	ATATGTGATGGGTTAAAAAGGATCGATCCTTAATCGCCACTTGAATCCTC	*X. doucetiae* DSM 17909^T
	GG144	CCAATGTCAATTTCATGAAATACCGTTCGATATCCATATATCCGATAGGTAGCATATAG	
	GG145	CTATATGCTACCTATCGGATATATGGATATCGAACGGTATTTCATGAAATTGAC	
	GG146	CAATTTGTGGAATTCCCGGGAGAGCTCGGTCATGAGCAGACGCCAG	
pEB17Δ*apeC*	GG241	ATATGTGATGGGTTAAAAAGGATCGATCCTGGATTTCACTCAAGACGTTTG	*X. doucetiae* DSM 17909^T
	GG242	GTAATATTGGCTGAAATCCTTTTCATCATCGAAATACCGTTCGTTACTGCTTC	
	GG243	CTGCAAGAAGCAGTAACGAACGGTATTTCGATGATGAAAAGGATTTCAGC	
	GG244	CAATTTGTGGAATTCCCGGGAGAGCTCCCCGTTTTCTGTATCAACC	
pEB17Δ*apeD*	GG167	ATATGTGATGGGTTAAAAAGGATCGATCCTGTTTTTACAGCATTGATGATTTTACC	*X. doucetiae* DSM 17909^T
	GG168	AACTCTTGCATCATCGTATCCGATATCTACTTATCGGCTCCAATTCCAC	
	GG169	GATCATTGTCAGTGGAATTGGAGCCGATAAGTAGATATCGGATACGATGATGCAAGAG	
	GG170	CAATTTGTGGAATTCCCGGGAGAGCTCGATAGTACATAAGAAGTTGATGATTGCG	
pEB17Δ*apeE*	GG147	ATATGTGATGGGTTAAAAAGGATCGATCCTGTTGCCATCTTGCACGTC	*X. doucetiae* DSM 17909^T
	GG148	CTTTTGTTTTTCCATGATGGCACCTGCTCCATCGTATCCGATATCTATTAGTTTG	
	GG149	CCGTCAAACTAATAGATATCGGATACGATGGAGCAGGTGCCATCATGG	
	GG150	CAATTTGTGGAATTCCCGGGAGAGCTCATCCTTTCAATGACAGGTGGC	
pEB17Δ*apeF*	GG151	ATATGTGATGGGTTAAAAAGGATCGATCCTGATGCAGAAACTTTGCTCCC	*X. doucetiae* DSM 17909^T
	GG152	CTGTTTGTTTTGCTGATGGTTTATGGCTGAGATGGCACCTGCTCTTATG	
	GG153	CAGAAAGCATAAGAGCAGGTGCCATCTCAGCCATAAACCATCAGC	
	GG154	CAATTTGTGGAATTCCCGGGAGAGCTCTCTTCCGATAGCCATTGG	
pEB17Δ*apeG*	GG187	ATATGTGATGGGTTAAAAAGGATCGATCCTTAGATATCGGATACGATGATGCAAGAG	*X. doucetiae* DSM 17909^T
	GG188	GATAGCCATTGGGAGATTGATCGTGCTTTTATTAACTACCCAAATGTTTGCTGTTTG	
	GG189	CAAAACAAACAGCAAACATTTGGGTAGTTAATAAAAGCACGATCAATCTCCC	
	GG190	CAATTTGTGGAATTCCCGGGAGAGCTCTGCGGAAAGTCAAACCATAC	
pEB17Δ*apeH*	GG211	ATATGTGATGGGTTAAAAAGGATCGATCCTGCAGTAAAAAATTGCTATGGC	*X. doucetiae* DSM 17909^T

	GG212	CATGTTGAGCAGGTTGCTCGCGGTGAATTTC AATGGAAATGAGCAACC	
	GG213	CTATTAATTGGGTTGCTCATTTCCATTGAAA TTCACCGCGAGCAAC	
	GG214	CAATTTGTGGAATTCCCGGGAGAGCTCATAT CAAAATCCATGCGACG	
pEB17Δ*apeI*	GG219	ATATGTGATGGGTTAAAAAGGATCGATCCTT CCTGCGTGATCAGATCC	*X. doucetiae* DSM 17909^T
	GG220	CCACGCAGGGCGTCATCGTATTCACGCTAAA TAGCTCCTGTAATGCAGGC	
	GG221	CTCATGGCCTGCATTACAGGAGCTATTTAGC GTGAATACGATGACGC	
	GG222	CAATTTGTGGAATTCCCGGGAGAGCTCCTTG CGTTCTTGAATATCTGAC	
pEB17Δ*apeJ*	GG155	ATATGTGATGGGTTAAAAAGGATCGATCCTG GCCTTTGCATTTTGCCTATG	*X. doucetiae* DSM 17909^T
	GG156	GCAGTAAAACGAGGATCAGTCAGCATTTTTA ACTTTATCTTTCCTTGGCTGG	
	GG157	CTGCCAGCCAAGGAAAGATAAAGTTAAAAA TGCTGACTGATCCTCG	
	GG158	CAATTTGTGGAATTCCCGGGAGAGCTCGCAT CAAGGTTAGCCTGACC	
pEB17Δ*apeK*	GG215	ATATGTGATGGGTTAAAAAGGATCGATCCTG TTGTTGGCTATTTCTGGG	*X. doucetiae* DSM 17909^T
	GG216	CAGAAACAGCAGTATCCCGCGCCATTTTTTT TTTTATTCCTTATTTGTCCG	
	GG217	CATCTGCCCGGACAAATAAGGAATAAAAAA AAAAATGGCGCGGGATAC	
	GG218	CAATTTGTGGAATTCCCGGGAGAGCTCGGAC TCACCATCCACACCAG	
pEB17Δ*apeL*	GG191	ATATGTGATGGGTTAAAAAGGATCGATCCTT ATTGCCGGTAACGGATG	*X. doucetiae* DSM 17909^T
	GG192	CCAGAATCGTGCCAGCAGACGTGGCGGCTT GACCCCCATGC	
	GG193	GATATTCTGTTTGAACGCATGGGGGTCAAGC CGCCACGTCTGCTGGCAC	
	GG194	CAATTTGTGGAATTCCCGGGAGAGCTCAATA CTGATGGATAGCACACACAGC	
pEB17Δ*apeM*	GG195	ATATGTGATGGGTTAAAAAGGATCGATCCTC GTGAATCCGGCTATGTTTG	*X. doucetiae* DSM 17909^T
	GG196	CAGGTCAGGGACAGGATGAATAACCGTAGG CTCAGCGTCTCTGGTG	
	GG197	GACACCAATTAACACCAGAGACGCTGAGCC TACGGTTATTCATCCTGTCCC	
	GG198	CAATTTGTGGAATTCCCGGGAGAGCTCGCTC CCGACCATGACG	
pEB17Δ*apeN*	GG199	ATATGTGATGGGTTAAAAAGGATCGATCCTA CGCAGAAAAAACGTTGCAAC	*X. doucetiae* DSM 17909^T
	GG200	CATACCTACGGCAGAAATATAAATCATGTTG ATTGCTTTTTCCTTTTTTGGC	
	GG201	GCCAAAAAAGGAAAAAGCAATCAACATGAT TTATATTTCTGCCG	
	GG202	CAATTTGTGGAATTCCCGGGAGAGCTCGCAG GTTGATATAACCTATCTCTG	

pEB17Δ*apeO*	GG159	ATATGTGATGGGTTAAAAAGGATCGATCCTG TGGTCATAGCCTGAACTTATTTTC	*X. doucetiae* DSM 17909^{T}
	GG160	ATAGCGATCCACGGGTAAATAGTCAGGCAG TTTTACTCTTCCAAATGCTGAATG	
	GG161	CGCCATTCAGCATTTGGAAGAGTAAAACTGC CTGACTATTTACCCGTGG	
	GG162	CAATTTGTGGAATTCCCGGGAGAGCTCTTGG TATGGATGACACTATCCCAG	
pEB17Δ*apeP*	GG223	ATATGTGATGGGTTAAAAAGGATCGATCCTA CCAGCAATCACATGGGTC	*X. doucetiae* DSM 17909^{T}
	GG224	GGCACCGGTCACGAGAACTGAACGCATTAA GCCACTCCCAATATCAGG	
	GG225	CCAGCCTGATATTGGGAGTGGCTTATGCGTT CAGTTCTCGTGAC	
	GG226	CAATTTGTGGAATTCCCGGGAGAGCTCCGAT AGCCAATCCTGTCCC	
pEB17Δ*apeQ*	GG227	ATATGTGATGGGTTAAAAAGGATCGATCCTC CATTGCAGCGATCAATATG	*X. doucetiae* DSM 17909^{T}
	GG228	CCTTTCCTGATGGGATGTCGCATTATGGCTA TGCTACTCCATCCTGTTTATTTATG	
	GG229	CTCATAAATAAACAGGATGGAGTAGCATAG CCATAATGCGACATCCC	
	GG230	CAATTTGTGGAATTCCCGGGAGAGCTCCCGT GGGCACTGATGTAAC	
pEB17Δ*apeR*	GG163	ATATGTGATGGGTTAAAAAGGATCGATCCTT TTGGCAGTTTTGAAGGTGAAATC	*X. doucetiae* DSM 17909^{T}
	GG164	GCTTTGTCAGCGGTCTTAACGCACTAAAAAG CATCCCTCCGTTGATTG	
	GG165	GGTCATCTCAATCAACGGAGGGATGCTTTTT AGTGCGTTAAGACCGCTG	
	GG166	CAATTTGTGGAATTCCCGGGAGAGCTCTAAA AGGGATCATCCCCTGAGT	
Oligonucleotides used for verification of *ape*+ mutants			
***ape*$^{+}$ mutant**	**Oligonucleotide 5` to 3`**		
Δ*apeB*	GG171	CTGCTGGCTAATCAATAAACATCCATGTTAAAGC	
	GG172	AAATCAGCAATAAATTAAACCAAATCAGGGAGAGTA	
Δ*apeC*	GG245	CATTACTGATCTGCAAGAAGCAGTAACGAACGG	
	GG246	GACGGTGTTAGTAATTGAGTAAGCTGGCGATTGAGTTGG	
Δ*apeD*	GG183	GAAACAGAACCCAGCCTTCCTCAAAG	
	GG184	CCTTTCAATGACAGGTGGCCCATAAC	
Δ*apeE*	GG173	CAATCGCCAGCTTACTCAATTACTAACACCG	
	GG174	ACTTTACGTGTATAGATAACGCCTTCTGGGGG	
Δ*apeF*	GG175	GTCAACACTTCACTTCTGTCGCTACACTGG	
	GG176	CTTACCCGCATGTAATGTTGCCAGCAG	
Δ*apeG*	GG203	AGCCATAAACCATCAGCAAAACAAACAGC	
	GG204	GCGATCAAATGGTAACCCCAGTGAC	
Δ*apeH*	GG231	GATTCAATCGATGCTCTGGAGCTGGG	
	GG232	TCATGTTGAGCAGGTTGCTCGCGG	
Δ*apeI*	GG235	CTGGCTGCTCTGTGGGGCGATAAGC	
	GG236	GATCACCACGCAGGGCGTCATC	
Δ*apeJ*	GG177	ACAACGGCAGCGAAGGCCAGACTG	
	GG178	CTCAGCGTCTCTGGTGTTAATTGGTGTCG	
Δ*apeK*	GG233	ACGCAAGCCCTTTGAGTGTCTGCTTTACC	

	GG234	CAAACTGGTTGTCAGAAACAGCAGTATCCC
Δ*apeL*	GG205	TCTGTTTGAACGCATGGGGGTCAAGC
	GG206	CCAACGTCACTACCGTTCCTGCCAGC
Δ*apeM*	GG207	CCGAGCTTGCTTTTACCCGACACC
	GG208	GCCAGATGTACTGGTGCCCATGATCACG
Δ*apeN*	GG209	CTATCCCCACTGGCCATGCCTGAGC
	GG210	CTGATTGATGACGATCGACTCCATCTGG
Δ*apeO*	GG179	CACAGAGATTCATTATGATGCCCCAAATGG
	GG180	TGCCCCGATAATACCGGCTTTCGC
Δ*apeP*	GG237	CCTTGATGAGGGTGATCAGCATGTCAGC
	GG238	ATCCCTTTGCTGGCACCGGTCAC
Δ*apeQ*	GG239	ACGCATGGCATATGTCAGCCCCG
	GG240	GGCCTTTCCTGATGGGATGTCGC
Δ*apeR*	GG181	CAAATGGAAGAAGCCGCCTTGAAAGAAG
	GG182	TCGGTGATTTTTCTCAACGACATACTTTGG

Table S3. Plasmids used in this study.

Plasmid	Genotype	Reference
pAL03	R6Kγ ori, oriT, *sacB*, *araC*, *ara*BAD, Km^r	[2]
pAL03_ape_mP	markerless promoter exchange plasmid based on pAL03 with 800 bp of up- and downstream region of *apeB* start codon, Km^r	[15]
pEB17_Km	R6Kγ ori, oriT, *araC*, *ara*BAD promoter, Km^r	[2]
pEB17Δ*apeB*	Deletion plasmid based on pEB17_Km with Km^r, with 800 bp of up- and downstream region of *apeB*	this work
pEB17Δ*apeC*	Deletion plasmid based on pEB17_Km with Km^r, with 761 bp of up- and 730 bp of downstream region of *apeC*	this work
pEB17Δ*apeD*	Deletion plasmid based on pEB17_Km with Km^r, with 850 bp of up- and downstream region of *apeD*	this work
pEB17Δ*apeE*	Deletion plasmid based on pEB17_Km with Km^r, with 650 bp of up- and downstream region of *apeE*	this work
pEB17Δ*apeF*	Deletion plasmid based on pEB17_Km with Km^r, with 650 bp of up- and downstream region of *apeF*	this work
pEB17Δ*apeG*	Deletion plasmid based on pEB17_Km with Km^r, with 600 bp of up- and downstream region of *apeG*	this work
pEB17Δ*apeH*	Deletion plasmid based on pEB17_Km with Km^r, with 956 bp of up- and 896 bp of downstream region of *apeH*	this work
pEB17Δ*apeI*	Deletion plasmid based on pEB17_Km with Km^r, with 826 bp of up- and 782 bp of downstream region of *apeI*	this work
pEB17Δ*apeJ*	Deletion plasmid based on pEB17_Km with Km^r, with 950 bp of up- and 983 bp of downstream region of *apeJ*	this work
pEB17Δ*apeK*	Deletion plasmid based on pEB17_Km with Km^r, with 850 bp of up- and 818 bp of downstream region of *apeK*	this work
pEB17Δ*apeL*	Deletion plasmid based on pEB17_Km with Km^r, with 857 bp of up- and 850 bp of downstream region of *apeL*	this work
pEB17Δ*apeM*	Deletion plasmid based on pEB17_Km with Km^r, with 855 bp of up- and 843 bp of downstream region of *apeM*	this work
pEB17Δ*apeN*	Deletion plasmid based on pEB17_Km with Km^r, with 850 bp of up- and 853 bp of downstream region of *apeN*	this work
pEB17Δ*apeO*	Deletion plasmid based on pEB17_Km with Km^r, with 850 bp of up- and 825 bp of downstream region of *apeO*	this work
pEB17Δ*apeP*	Deletion plasmid based on pEB17_Km with Km^r, with 823 bp of up- and 820 bp of downstream region of *apeP*	this work
pEB17Δ*apeQ*	Deletion plasmid based on pEB17_Km with Km^r, with 894 bp of up- and 934 bp of downstream region of *apeQ*	this work
pEB17Δ*apeR*	Deletion plasmid based on pEB17_Km with Km^r, with 830 bp of up- and downstream region of *apeR*	this work

Table S4. *ape* BGC from *X. doucetiae* DSM17909 (genome accession number VNHN00000000, NCBI GenBank: NZ_FO704550.1) with predicted (NCBI blastp) and experimentally confirmed gene functions.[15]

gene	Locus tag	Protein ID	(predicted) function
apeA	XDD1_RS15980	WP_045972701.1	hypothetical protein
apeB	XDD1_RS15985	WP_045972703.1	SAM dependent methyltransferase
apeC	XDD1_RS15990	WP_045972706.1	chain length factor (CLF)
apeD	XDD1_RS15995	WP_045972707.1	glycerol-3-phosphate AT
apeE	XDD1_RS16000	WP_045972709.1	acyl-carrier protein (ACP)
apeF	XDD1_RS16005	WP_071827286.1	ACP
apeG	XDD1_RS16010	WP_052705766.1	COG4648 membrane protein
apeH	XDD1_RS16015	WP_045972716.1	acyl-ACP synthetase (AasS)
apeI	XDD1_RS16020	WP_045972718.1	dehydratase (DH)
apeJ	XDD1_RS16025	WP_045972720.1	glycosy/acyltransferase
apeK	XDD1_RS16030	WP_045972722.1	acyl-CoA thioesterase (TE)
apeL	XDD1_RS16035	WP_045973732.1	outer membrane lipoprotein carrier LolA
apeM	XDD1_RS16040	WP_045972724.1	MMPL transporter
apeN	XDD1_RS16045	WP_045972727.1	DUF3261 protein
apeO	XDD1_RS16050	WP_045972729.1	ketosynthase (KS)
apeP	XDD1_RS16055	WP_045973733.1	DH
apeQ	XDD1_RS16060	WP_045972731.1	ketoreductase (KR)
apeR	XDD1_RS16065	WP_045972733.1	KS

Table S5. Conditions for analytical HPLC/MS for APEL detection.

Condition overview				
compound	column	solvent system[6]	LC-condition	MS-parameter
APEL	C3	A:MeCN/2-propanol(9:1)/ B:MeCN/H2O(6:4) +0.2 % formic acid +10 mM ammonium formate	Gradient I	APEL-HPLC-MS
	C18AX		Gradient II	

Columns	
C3	Zorbax 300SB-C3 300Å (Agilent), 150 mm x 3.0 mm x 3.5 µm
	No separation of APEL isomers
C18AX	Atlantis C18AX (Waters), 50 mm x 2.1 mm x 1.7 µm
	Leads to additional separation of APEL isomers

LC-conditions			
Gradient I	flow rate 1.2 mL/min, column oven temperature 55°C		
	min	solvent A (%)	solvent B (%)
	0.0	80	20
	1.0	80	20
	10.0	47	53
	10.1	0	100
	14.0	0	100
	14.1	80	20
	16.0	80	20
Gradient II	flow rate 0.8 mL/min, column oven temperature 55°C		
	min	solvent A (%)	solvent B (%)
	0.0	32	68
	1.0	32	68
	4.0	53	47
	12.0	56	44
	12.1	97	3
	16.0	97	3
	16.1	32	68
	20.0	32	68

MS-parameter IMPACT II		
	Source	Tune
APEL HPLC-MS	End Plate Offset 500 V Capillary 4500 V Nebulizer 3.0 Bar Dry Gas 8 L/min Dry Temp 200°C	<u>Transfer</u> Funnel1 RF 300 Vpp Funnel2 RF 300 Vpp Hexapole RF 60 Vpp <u>Quadrupole</u> Ion Energy 5 eV <u>Collision Cell</u> Collision Energy 10.0 eV Pre Pulse Storage 5 µs Stepping Collision RF 800 Vpp Stepping Transfer Time 140 µs

Table S6. Culture conditions for the isolation of APELs.

compound	strain	culture volume	cultivation conditions
APEL-1284 (**1**), 1270 (**2**), 1256a (**3**), 1242 (**4**)	*ape*$^+$	80 L LB (4X 20 L, fermenter)	2 d, 30 °C, 160 rpm, 4 L O_2/h

Table S7. Chromatography conditions for the isolation of APELs.

compound	chromatography	column	solvent system	LC-parameter
APELs	normal phase	silica gel	A: chloroform B: PL-polar*	silica gel
APEL- 1284 (**1**) 1270 (**2**) 1256a (**3**) 1242 (**4**)	reversed-phase/anion exchange analytical	C18/AX	A: 2-propanol/MeCN (9:1) B: MeCN/H_2O(6:4) +0.2% FA +10 mM ammonium formate	Gradient I
APEL-1284 (**1**)	reversed-phase/anion exchange analytical	C18/AX	A: 2-propanol/MeCN (9:1) B: MeCN/H_2O(6:4) +0.2% FA +10 mM ammonium formate	Gradient II -1284
APEL-1270 (**2**)				Gradient II -1270
APEL-1256a (**3**)				Gradient II -1256a
APEL-1242 (**4**)				Gradient II -1242

*PL-polar: 25:25:10:7 ethyl acetate/2-propanol/methanol/0.25% KCl aqu.

Table S8. Column specifications and chromatography parameters used for the isolation process of APEL.

Columns				
Silica gel	SNAP KP-Sil 100 g			
C18/AX	Atlantis C18AX (Waters), 4.6 x 250 mm x 5µm			
LC-parameter				
normal phase **Silica gel**	Chromatographic system: Biotage Flash-SP1			
	flow rate 50 mL/min, RT			
	solvent A: chloroform, solvent B: PL-polar*, 1. Wash: 50% PL-polar, 60-80 CV; Elution APEL: 75% PL-polar, 15 CV 2. Wash: 40% PL-polar, 60-80 CV Elution APEL, gradient 50-85% PL-polar, 60 CV			
reversed-phase **Gradient I**	Chromatographic system: Agilent 1260 Infinity or Agilent 1260 Infinity II LC/MSD			
	column oven temperature 40°C			
	min	solvent A (%)	solvent B (%)	flow rate (mL/min)
	4.0	39	61	1.5
	52.0	39	61	1.5
	52.1	3	97	2.0
	58.0	3	97	2.0
	58.1	39	61	2.0
	63.0	39	61	2.0
reversed-phase **Gradient II-1242**	min	solvent A (%)	solvent B (%)	flow rate (mL/min)
	4.0	39	61	1.5
	42.0	39	61	1.5
	42.1	3	97	2.0
	48.0	3	97	2.0
	48.1	39	61	2.0

	61.0	39	61	2.0
reversed-phase **Gradient II-1256a**	min	solvent A (%)	solvent B (%)	flow rate (mL/min)
	4.0	39	61	1.5
	44.0	39	61	1.5
	44.1	3	97	2.0
	50.0	3	97	2.0
	50.1	39	61	2.0
	55	39	61	2.0
reversed-phase **Gradient II-1270**	min	solvent A (%)	solvent B (%)	flow rate (mL/min)
	4.0	39	61	1.5
	48.0	39	61	1.5
	48.1	3	97	2.0
	50.0	3	97	2.0
	50.1	39	61	2.0
	55	39	61	2.0
reversed-phase **Gradient II-1284**	min	solvent A (%)	solvent B (%)	flow rate (mL/min)
	4.0	39	61	1.5
	48.0	39	61	1.5
	48.1	3	97	2.0
	50.0	3	97	2.0
	50.1	39	61	2.0
	55	39	61	2.0

*PL-polar: 25:25:10:7 ethyl acetate/2-propanol/methanol/0.25% KCl aqu.

Table S9. HR-MS fragment ions derived from direct infusion MR-MS (for APEL-1256b (**5**)**,** HPLC-Impact II-MS was used) measurements of APELs with the corresponding sum formula prediction. cFA, conjugated fatty acyl. GalNAc, *N*-acetylgalactosamine. Pseudo-molecular ions of APELs **1**-**4** were determined using HPLC-Impact II-MS.

building block	**sum formula** [M]	**calculated mass** $[M]^+$	**detected mass** $[M]^+$	**Δppm**
APEL-1242 (**4**)				
parent mass $[M\text{-}H_2O+H]^+$	$C_{71}H_{104}NO_{15}P$	1242.721634	1242.721517	0.095
APE	$C_{20}H_{19}O_2$	291.13796	291.13804	0.3
cFA	$C_{26}H_{39}O$	367.29954	367.29965	0.3
myristoyl	$C_{14}H_{27}O$	211.20564	211.20570	0.3
APE-GalNAc	$C_{28}H_{32}NO_7$	494.31733	494.21739	0.1
glycerol-cFA-myristoyl	$C_{43}H_{71}O_4$	651.53469	651.53469	0.1
glycerol-myristoyl	$C_{17}H_{33}O_3$	285.24242	285.24251	0.3
glycerol-myristoyl-phosphate	$C_{17}H_{34}O_6P$	365.20875	365.20885	0.3
GalNAc	$C_6H_8NO_2$	126.05496	126.20550	0.3
	$C_8H_{10}NO_3$	168.06552	168.06557	0.3
	$C_8H_{12}NO_4$	186.07608	186.07614	0.3
	$C_8H_{14}NO_5$	204.08665	204.08671	0.3
GalNAc-phosphate*		176.00782	176.00861	4.5
		133.99864	133.99799	4.8
phosphate*		97.97679	97.97688	0.9
APEL-1256a (**3**)				
parent mass $[M\text{-}H_2O+H]^+$	$C_{72}H_{106}NO_{15}P$	1256.737284	1256.737787	0.399
APE	$C_{21}H_{21}O_2$	305.15306	305.15368	0.2
cFA	$C_{26}H_{39}O$	367.29954	367.29963	0.3
myristoyl	$C_{14}H_{27}O$	211.20564	211.20570	0.3
APE-GalNAc	$C_{29}H_{34}NO_7$	508.23298	508.23301	0.1
glycerol-cFA-myristoyl	$C_{43}H_{71}O_4$	651.53469	651.53470	0.0
glycerol-myristoyl	$C_{17}H_{33}O_3$	285.24242	285.24250	0.3
glycerol-myristoyl-phosphate	$C_{17}H_{34}O_6P$	365.20875	365.20884	0.2
GalNAc	$C_6H_8NO_2$	126.05496	126.05498	0.2
	$C_8H_{10}NO_3$	168.06552	168.06556	0.2
	$C_8H_{12}NO_4$	186.07608	186.07613	0.2
	$C_8H_{14}NO_5$	204.08665	204.08670	0.3
GalNAc-phosphate*		176.00782	176.00851	3.9
		133.99864	133.99793	5.3
phosphate*		97.97679	97.97677	0.3
APEL-1256b (**5**)				
parent mass $[M\text{-}H_2O+H]^+$	$C_{72}H_{106}NO_{15}P$	1256.7373	1256.7359	1.1
APE	$C_{19}H_{17}O_2$	277.1223	277.1227	1.4
cFA	$C_{26}H_{39}O$	367.2995	367.2987	0.8
palmitoyl	$C_{16}H_{31}O$	239.2369	239.2371	0.7
APE-GalNAc	$C_{27}H_{30}NO_7$	480.2017	480.2011	1.3
glycerol-cFA- palmitoyl	$C_{45}H_{75}O_4$	679.5660	n.d.	-
glycerol-palmitoyl	$C_{19}H_{37}O_3$	313.2737	313.2736	0.4
glycerol-palmitoyl-phosphate	$C_{19}H_{37}O_3P$	393.2401	393.2431	13.3
GalNAc	$C_6H_8NO_2$	126.0550	126.0565	12.0
	$C_8H_{10}NO_3$	168.0655	168.0655	0.3
	$C_8H_{12}NO_4$	186.0761	186.0775	7.5
	$C_8H_{14}NO_5$	204.0867	204.0862	2.1
GalNAc-phosphate*		176.0078	n.d.	-
		133.9986	n.d.	-
phosphate*		97.9768	n.d.	-
APEL-1270 (**2**)				

parent mass $[M-H_2O+H]^+$	$C_{73}H_{108}NO_{15}P$	1270.752934	1270.752954	0.015
APE	$C_{20}H_{19}O_2$	291.13796	291.13803	0.3
cFA	$C_{26}H_{39}O$	367.29954	367.29967	0.4
palmitoyl	$C_{16}H_{31}O$	239.23690	239.23701	0.3
APE-GalNAc	$C_{28}H_{32}NO_7$	494.31733	494.21738	0.1
glycerol-cFA- palmitoyl	$C_{45}H_{75}O_4$	679.56599	679.56598	0.0
glycerol-palmitoyl	$C_{19}H_{37}O_3$	313.27372	313.27338	0.3
glycerol-palmitoyl-phosphate	$C_{19}H_{37}O_3P$	393.24005	393.24018	0.3
GalNAc	$C_6H_8NO_2$	126.05496	126.054982	0.2
	$C_8H_{10}NO_3$	168.06552	168.06556	0.2
	$C_8H_{12}NO_4$	186.07608	168.07613	0.2
	$C_8H_{14}NO_5$	204.08665	204.086703	0.3
GalNAc-phosphate*		176.00782	176.00864	4.7
		133.99864	133.99784	6.0
phosphate*		97.97679	97.97673	0.7
APEL-1284 (**1**)				
parent mass $[M-H_2O+H]^+$	$C_{74}H_{110}NO_{15}P$	1284.768584	1284.768584	0.001
APE	$C_{21}H_{21}O_2$	305.15306	305.15366	0.2
cFA	$C_{26}H_{39}O$	367.29954	367.29909	1.2
palmitoyl	$C_{16}H_{31}O$	239.23690	239.23699	0.2
APE-GalNAc	$C_{29}H_{34}NO_7$	508.23298	508.23299	0.2
glycerol-cFA- palmitoyl	$C_{45}H_{75}O_4$	679.56599	679.56594	0.0
glycerol-palmitoyl	$C_{19}H_{37}O_3$	313.27372	313.27379	0.2
glycerol-palmitoyl-phosphate	$C_{19}H_{38}O_6P$	393.24005	393.24017	1.1
GalNAc	$C_6H_8NO_2$	126.05496	126.05498	0.2
	$C_8H_{10}NO_3$	168.06552	168.06555	0.2
	$C_8H_{12}NO_4$	186.07608	186.07612	0.2
	$C_8H_{14}NO_5$	204.08665	204.08670	0.2
GalNAc-phosphate*		176.00782	176.00840	3.3
		133.99864	133.99768	7.1
phosphate*		97.97679	97.97665	1.5
pseudo-molecular ions of APEL-1242 (**4**), neutral sum formula: $C_{71}H_{106}NO_{16}P$				
pseudo-ion		**calculated mass**	**detected mass**	**Δppm**
$[M+H]^+$		1260.7322	1260.7359	2.9
$[M-H_2O+H]^+$		1242.7216	1242.7191	2.0
$[M+NH_4]^+$		1277.7587	1277.7556	2.4
$[M+Na]^+$		1282.7141	1282.7119	1.7
$[M+Na_2-H]^+$		1304.6961	1304.6930	2.4
pseudo-molecular ions of APEL-1256a (**3**), neutral sum formula: $C_{72}H_{108}NO_{16}P$				
pseudo-ion		**calculated mass**	**detected mass**	**Δppm**
$[M+H]^+$		1274.7479	1274.7515	2.8
$[M-H_2O+H]^+$		1256.7373	1256.7355	1.4
$[M+NH_4]^+$		1291.7744	1291.7709	2.7
$[M+Na]^+$		1296.7298	1296.7277	1.6
$[M+Na_2-H]^+$		1318.7117	1318.7100	1.3
pseudo-molecular ions of APEL-1270 (**2**), neutral sum formula: $C_{73}H_{110}NO_{16}P$				
pseudo-ion		**calculated mass**	**detected mass**	**Δppm**
$[M+H]^+$		1288.7635	1288.7654	1.5
$[M-H_2O+H]^+$		1270.7529	1270.7486	3.4
$[M+NH_4]^+$		1305.7900	1305.7847	4.0
$[M+Na]^+$		1310.7454	1310.7404	3.8
$[M+Na_2-H]^+$		1332.7274	1332.7237	2.8

pseudo-molecular ions of APEL-1284 (**1**), neutral sum formula: $C_{74}H_{112}NO_{16}P$			
pseudo-ion	**calculated mass**	**detected mass**	**Δppm**
$[M+H]^+$	1302.7792	1302.7816	1.8
$[M-H_2O+H]^+$	1284.7686	1284.7644	3.3
$[M+NH_4]^+$	1319.8057	1319.8014	3.3
$[M+Na]^+$	1324.7611	1324.7560	3.8
$[M+Na_2-H]^+$	1346.7430	1346.7406	1.8

*detected as neutral loss, n.d. = not detectable

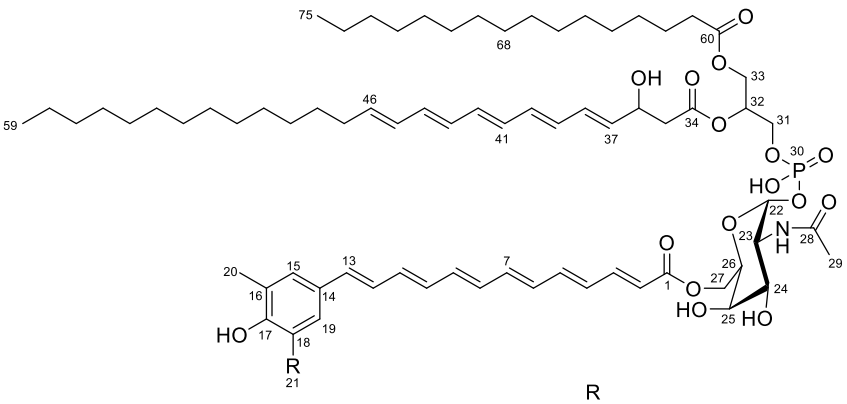

Table S10. ^{1}H (950 MHz) NMR data assignments for APEL-1284 (**1**) and ^{1}H (950 MHz), ^{13}C (239 MHz), and ^{31}P (243 MHz) NMR data assignments for APEL-1270 (**2**) in DMF-d_7 (NMR spectra see Figs. S18-27 for **1**; Figs. S28-41 for **2**).

	No.	APEL-1284 (**1**)	APEL-1270 (**2**)		
		δ_H (mult., *J*)	δ_H (mult., *J*)	δ_C, mult.	δ_P
aryl polyene					
	1	-	-	169.2, C	-
	2	6.03 (d, 15.1)	6.03 (d, 15.2)	122.7, CH	-
	3	7.40 (dd, 14.8, 11.5)	7.40 (dd, 14.6, 11.6)	147.6, CH	-
	4	6.54 (dd, 14.6, 11.5)	6.54 (dd, 14.6, 11.6)	132.6, CH	-
	5	6.87 (ov)	6.88 (ov, 14.6, 11.5)[a]	144.3, CH	-
	6	6.48 (ov)	6.47 (td, 14.6, 11.5)	134.8, CH	-
	7	6.66 (dd, 14.7, 11.3)	6.65 (dd, 14.7, 11.4)	140.7, CH	-
	8	6.48 (ov)	6.47 (td, 14.6, 11.5)	134.6, CH	-
	9	6.58 (ov)	6.57 (ov, 14.8, 10.9)[a]	139.2, CH	-
	10	6.48 (ov)	6.47 (td, 14.6, 11.5)	134.3, CH	-
	11	6.58 (ov)	6.57 (ov, 14.8, 10.9)[a]	138.7, CH	-
	12	6.87 (ov)	6.85 (ov, 15.5, 10.7)[a]	128.7, CH	-
	13	6.58 (ov)	6.61 (d, 15.5)	137.0, CH	-
	14	-	-	131.7, C	-
	15	7.13 (br s)	7.28 (d, 1.6)	131.7, CH	-
	16	-	-	127.2, C	-
	17	-	-	159.3, C	-
	18	-	6.89 (d, 8.2)	117.7, CH	-
	19	7.13 (br s)	7.18 (dd, 8.2, 1.7)	128.3, CH	-
	20	2.24 (s)	2.18 (s)	18.3, CH_3	-
	21	2.24 (s)	-	-	-
N-acetyl-α-galactosamine					
	22	5.47 (dd, 7.6, 2.8)	5.48 (dd, 7.6, 2.9)	96.6, CH	-
	23	4.21 (ov)	4.21 (ov, 10.7, 3.5)[a]	54.1, CH	-
	23NH	8.83 (d, 7.2)	8.79 (d, 7.0)	-	-
	24	3.84 (dd, 10.6, 3.1)	3.86 (dd, 10.7, 2.9)	72.0, CH	-
	25	3.90 (br s)	3.90 (d, 2.9)	71.6, CH	-
	26	4.23 (ov)	4.23 (ov, 12.2, 1.8)[a]	72.3, CH	-
	27	4.32 (br d, 6.8)	4.31 (br d, 6.0)	66.9, CH_2	-
	28	-	-	174.3, C	-
	29	1.91 (s)	1.91 (s)	24.9, CH_3	-
phosphate					

	30	-	-	-	–1.42
glycerol					
	31	4.08 (m)	4.08 (dd, 11.4, 4.2)	65.7, CH_2	-
		3.97 (m)	3.98 (dd, 11.4, 3.8)		
	32	5.16 (br dt, 8.3, 4.5)	5.16 (br dt, 7.9, 4.4)	74.0, CH	-
	33	4.37 (dd, 11.9, 3.5)	4.37 (dd, 11.8, 3.5)	65.3, CH_2	-
		4.27 (dd, 11.9, 7.4)	4.27 (dd, 11.8, 7.4)		
conjugated fatty acyl					
	34	-	-	173.3, C	-
	35	2.53 (m)	2.53 (m)	45.8, CH_2	-
	36	4.59 (br dd, 12.0, 5.8)	4.59 (br dd, 11.9, 5.7)	70.8, CH	-
	37	5.84 (dd, 15.1, 5.8)	5.84 (dd, 15.2, 5.7)	139.6, CH	-
	38	6.39 (dd, 15.0, 10.8)	6.39 (dd, 14.6, 10.9)	132.2, CH	-
	39	6.30 (ov)	6.30 (ov, 14.6, 10.9)[a]	135.2, CH	-
	40	6.33 (ov)	6.33 (ov)	135.6, CH	-
	41	6.30 (ov)	6.30 (ov, 14.6, 10.9)[a]	135.2, CH	-
	42	6.33 (ov)	6.33 (ov)	136.0, CH	-
	43	6.25 (ov)	6.25 (ov, 14.7, 10.1)[a]	133.8, CH	-
	44	6.28 (ov)	6.28 (ov, 15.1, 10.6)[a]	136.2, CH	-
	45	6.12 (dd, 15.1, 10.3)	6.13 (dd, 15.1, 10.2)	133.6, CH	-
	46	5.75 (m)	5.75 (dt, 14.5, 7.2)	138.3, CH	-
	47	2.10 (m)	2.08 (dd, 14.9, 7.8)	35.4, CH_2	-
	48	1.37 (ov)	1.36 (ov)	31.7, CH_2	-
	49	1.55 (ov)	1.55 (ov)	27.5, CH_2	-
	50-56	1.27 (ov)	1.27 (ov)	32.2, CH_2	-
	57	1.27 (ov)	1.27 (ov)	34.4, CH_2	-
	58	1.27 (ov)	1.27 (ov)	25.1, CH_2	-
	59	0.86 (ov)	0.87 (ov)	16.3, CH_3	-
palmitoyl					
	60	-	-	175.6, C	-
	61	2.30 (m)	2.30 (t, 7.4)	36.3, CH_2	-
	62	1.55 (ov)	1.55 (ov)	27.5, CH_2	-
	63	1.37 (ov)	1.36 (ov)	31.7, CH_2	-
	64-72	1.27 (ov)	1.27 (ov)	32.2, CH_2	-
	73	1.27 (ov)	1.27 (ov)	34.4, CH_2	-
	74	1.27 (ov)	1.27 (ov)	25.1, CH_2	-
	75	0.86 (ov)	0.87 (ov)	16.3, CH_3	-

[a]Coupling constants extracted from DQF-COSY.

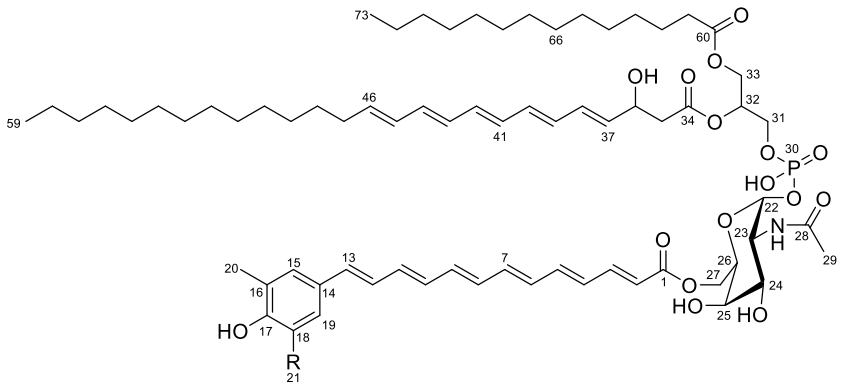

	R
APEL-1256a (**3**)	CH_3
APEL-1242 (**4**)	H

Table S11. ^{1}H (800 MHz) NMR data assignments for APEL-1256a (**3**) and ^{1}H (800 MHz), ^{13}C (200 MHz), and ^{31}P (243 MHz) NMR data assignments for APEL-1242 (**4**) and in DMF-d_7 (NMR spectra see Figs. S42-46 for **3**; Figs. S47-61).

	No.	APEL-1256a (**3**)	APEL-1242 (**4**)		
		δ_H (mult., *J*)	δ_H (mult., *J*)	δ_C, mult.	δ_P
aryl polyene					
	1	-	-	169.2, C	-
	2	6.03 (d, 15.2)	6.03 (d, 15.1)	122.7, CH	-
	3	7.40 (dd, 14.7, 11.3)	7.40 (dd, 15.1, 11.5)	147.6, CH	-
	4	6.54 (dd, 14.4, 11.9)	6.54 (dd, 14.5, 11.5)	132.6, CH	-
	5	6.87 (ov)	6.88 (ov)	144.3, CH	-
	6	6.47 (dd, 14.5, 11.0)	6.47 (ddd, 14.6, 11.6, 3.4)	134.9, CH	-
	7	6.66 (m)	6.66 (dd, 14.6, 11.2)	140.7, CH	-
	8	6.47 (dd, 14.5, 11.0)	6.47 (ddd, 14.6, 11.6, 3.4)	134.7, CH	-
	9	6.59 (ov)	6.58 (ov)	139.1, CH	-
	10	6.47 (dd, 14.5, 11.0)	6.47 (ddd, 14.6, 11.6, 3.4)	134.4, CH	-
	11	6.58 (ov)	6.58 (ov)	138.7, CH	-
	12	6.87 (ov)	6.88 (ov)	128.7, CH	-
	13	6.61 (ov)	6.62 (d, 15.5)	136.9, CH	-
	14	-	-	131.2, C	-
	15	7.14 (br s)	7.29 (d, 1.2)	131.8. CH	-
	16	-	-	127.2, C	-
	17	-	-	159.1, C	-
	18	-	6.86 (d, 8.4)	117.6, CH	-
	19	7.14 (br s)	7.20 (dd, 8.4, 1.6)	128.3, CH	-
	20	2.24 (s)	2.19 (s)	18.2, CH_3	-
	21	2.24 (s)	-	-	-
N-acetyl-α-D-galactosamine					
	22	5.46 (dd, 7.5, 2.9)	5.47 (dd, 7.6, 3.8)	96.5, CH	-
	23	4.23 (ov)	4.22 (ov)	54.2, CH	-
	23NH	8.98 (d, 7.0)	8.88 (d, 7.5)	-	
	24	3.83 (dd, 10.5, 3.0)	3.83 (ov)	72.5, CH	-
	25	3.89 (br s)	3.89 (ov)	71.6, CH	-
	26	4.23 (m)	4.23 (ov)	72.2, CH	-
	27	4.32 (br d, 4.9)	4.32 (ov)	66.9, CH_2	-
	28	-	-	174.4, C	-
	29	1.91 (s)	1.91 (s)	24.9, CH_3	-
phosphate					

	30	-	-	-	–1.41
glycerol					
	31	4.10 (m)	4.08 (m)	65.7, CH_2	-
		3.97 (m)	3.98 (m)		
	32	5.15 (m)	5.16 (br dt, 8.4, 4.7)	74.0, CH	-
	33	4.37 (dd, 11.9, 3.5)	4.37 (dd, 11.9, 3.6)	65.3, CH_2	-
		4.27 (dd, 11.9, 7.4)	4.27 (m)		
conjugated fatty acyl					
	34	-	-	173.3, C	-
	35	2.52 (m)	2.53 (m)	45.9, CH_2	-
	36	4.60 (m)	4.60 (br dd, 12.3, 6.4)	70.8, CH	-
	37	5.84 (dd, 15.3, 5.5)	5.84 (dd, 15.1, 5.8)	139.6, CH	-
	38	6.38 (dd, 15.3, 11.0)	6.38 (dd, 15.1, 10.7)	132.2, CH	-
	39	6.32 (ov)	6.32 (ov)	135.2, CH	-
	40	6.32 (ov)	6.32 (ov)	135.6, CH	-
	41	6.26 (ov)	6.26 (ov)	135.2, CH	-
	42	6.26 (ov)	6.26 (ov)	136.0, CH	-
	43	6.27 (ov)	6.27 (ov)	133.8, CH	-
	44	6.27 (ov)	6.27 (ov)	136.2, CH	-
	45	6.13 (m)	6.13 (dd, 15.1, 10.1)	133.6, CH	-
	46	5.75 (m)	5.76 (m)	138.3, CH	-
	47	2.09 (m)	2.08 (dd, 14.4, 7.1)	35.3. CH_2	-
	48	1.37 (ov)	1.37 (ov)	31.7, CH_2	-
	49	1.56 (ov)	1.55 (ov)	27.7, CH_2	-
	50-56	1.27 (ov)	1.27 (ov)	32.2, CH_2	-
	57	1.27 (ov)	1.27 (ov)	34.4, CH2	-
	58	1.27 (ov)	1.27 (ov)	25.1, CH_2	-
	59	0.86 (ov)	0.87 (ov)	16.3, CH_3	-
myristoyl					
	60	-	-	175.6, C	-
	61	2.31 (t, 7.4)	2.31 (t, 7.4)	36.3, CH_2	-
	62	1.56 (ov)	1.55 (ov)	27.7, CH_2	-
	63	1.37 (ov)	1.37 (ov)	31.7, CH_2	-
	64-70	1.27 (ov)	1.27 (ov)	32.2, CH_2	-
	71	1.27 (ov)	1.27 (ov)	34.4, CH2	-
	72	1.27 (ov)	1.27 (ov)	25.1, CH_2	-
	73	0.86 (ov)	0.87 (ov)	16.3, CH_3	-

Supplementary References

[1] C. Fu, W. P. Donovan, O. Shikapwashya-Hasser, X. Ye, R. H. Cole, *PLoS One* **2014**, *9*, e115318.
[2] E. Bode, A. O. Brachmann, C. Kegler, R. Simsek, C. Dauth, Q. Zhou, M. Kaiser, P. Klemmt, H. B. Bode, *ChemBiochem* **2015**, *16*, 1115.
[3] D. Reimer, F. I. Nollmann, K. Schultz, M. Kaiser, H. B. Bode, *J. Nat. Prod.* **2014**, *77*, 1976.
[4] H. B. Bode, M. W. Ring, G. Schwär, R. M. Kroppenstedt, D. Kaiser, R. Müller, *J Bacteriol* **2006**, *188*, 6524.
[5] A. A. Entezami, B. J. Venables, K. E. Daugherty, *J. Chrom. A* **1987**, *387*, 323.
[6] T. Cajka, O. Fiehn, *Metabolomics* **2016**, *12*, 34.
[7] C. G. Juo, S. W. Chen, G. R. Her, *Analytica Chimica Acta* **1995**, *311*, 153.
[8] K. Blin, M. H. Medema, R. Kottmann, S. Y. Lee, T. Weber, *Nucleic Acids Res.* **2017**, *45*, D555-D559.
[9] K. Katoh, D. M. Standley, *Mol Biol Evol* **2013**, *30*, 772.
[10] M. N. Price, P. S. Dehal, A. P. Arkin, *PLoS One* **2010**, *5*, e9490.
[11] R. D. Finn, P. Coggill, R. Y. Eberhardt, S. R. Eddy, J. Mistry, A. L. Mitchell, S. C. Potter, M. Punta, M. Qureshi, A. Sangrador-Vegas et al., *Nucleic Acids Res.* **2016**, *44*, D279-85.
[12] R. D. Finn, J. Clements, S. R. Eddy, *Nucleic Acids Res.* **2011**, *39*, W29-37.
[13] I. Letunic, P. Bork, *Bioinformatics* **2007**, *23*, 127.
[14] E. Bode, Y. He, T. D. Vo, R. Schultz, M. Kaiser, H. B. Bode, *Environ. Microbiol.* **2017**, *19*, 4564.
[15] Grammbitter, Gina L. C., M. Schmalhofer, K. Karimi, Y.-M. Shi, T. A. Schöner, N. J. Tobias, N. Morgner, M. Groll, H. B. Bode, *J. Am. Chem. Soc.* **2019**, *141*, 16615.
[16] S. Thoma, M. Schobert, *FEMS Microbiol. Lett.* **2009**, *294*, 127.